PLACE IN RETURN BOX to remove this checkout from your record.
TO AVOID FINES return on or before date due.

DATE DUE	DATE DUE	DATE DUE
SEP 1 9 2005		

MSU Is An Affirmative Action/Equal Opportunity Institution

GEOCHEMISTRY OF THE UNNAMED FORMATION
A CENTRAL VOLCANIC COMPLEX OF KEWEENAWAN AGE

By

Michael Patrick McDermott

A THESIS

Submitted to
Michigan State University
in partial fulfillment of the requirements
for the degree of

MASTER OF SCIENCE

Department of Geology

1990

ABSTRACT

GEOCHEMISTRY OF THE UNNAMED FORMATION
A CENTRAL VOLCANIC COMPLEX OF KEWEENAWAN AGE

By

Michael Patrick McDermott

The Unnamed Formation (UF) is located in the Lake Superior Region of Michigan. It represents the waning stages of volcanism associated with the Mid Continent Rift in Michigan. The UF is comprised of basalt, andesite, and felsite lava flows interbedded with subordinate sedimentary rocks.

The basalts and andesites are relatively evolved lavas (Mg & Ni depleted). The variation within the basalts and andesites can primarily be attributted to the fractional crystallization of olivine, pyroxene, and plagioclase. The basalt and andesite trace element distributions cannot be explained by simple crystal fractionation, and require up to 30% magma mixing with a rhyolitic magma such as those present within the UF.

The rhyolites of the UF contain up to 76% SiO_2. The variation present within the rhyloites is consistent with partial melting of more than one source. The rhyolites of the UF were likely formed due to wholesale or partial melting of the crust as it was heated by injection of the basaltic magma.

DEDICATION

This thesis is dedicated to the memory of John T. Wilband, teacher and friend. Thanks for believing in me John. You are missed.

ACKNOWLEDGMENTS

I would like to thank all of the people who have stood by me during this long and arduous task. First, my parents and family, including A. Laura & U. Howard and A. Glad & U. Jack, through the years they have all been politely inquisative as to the progress of this paper, but always supportive in both words and deeds. I won't forget the field work U. Howard!

Then there are the professors from whom I have garnered a great deal of knowledge. John, Tom Vogel, Dave Long, Bill Cambrey, and Jim Trow thanks. I may forget the content but I'll never forget your desire's to expand your knowledge, and the ability you gave me to do the same for myself; o.k. you to Duncan (have to appease the soft rockers). Graham, only one class, but it got me a job!

Last but not least there are the people who have made this whole process bearable by providing releases from the thesis induced anxiety, a living, or both. Mike thanks!, Jeff Pincumbe, Bob Hilty, Ed Everett, Bob Minning, Mark Allen, Lisa, Lars, Mo, Diane, and Michelle, you have all provided inspiration, help and respite thank you. There are many others who have contributed to this effort. Thank You!

TABLE OF CONTENTS

LIST OF FIGURES

LIST OF FIGURES
(Continued)

APPENDICES

GEOCHEMISTRY OF THE UNNAMED FORMATION
A CENTRAL VOLCANIC COMPLEX OF KEWEENAWAN AGE

INTRODUCTION

The Unnamed Formation (UF) is located in the Lake Superior Region of Michigan, U.S.A. (Figure 1) and is part of the Keweenawan volcanic and intrusive rocks of the Lake Superior region. The Keweenawan igneous rocks have been the subject of considerable geologic interest for over a century. In many cases, however, knowledge of these rocks is limited to preliminary characterization of the various major rock units exposed within the Lake Superior Basin. A compilation of work summarized in G.S.A. Memoir 156 "GEOLOGY AND TECTONICS OF THE LAKE SUPERIOR BASIN" edited by Wold and Hinze (1982), presents data and interpretations that serve as an evolving model of Keweenawan magmatic and tectonic activity.

They conclude that an "...integrated, multidisciplinary approach in which each geologic discipline built upon the results of previous studies, has led to the acceptance of the theory that the Lake Superior Basin is a surface manifestation of a major crustal rift. Questions that remain concerning the geologic history of the basin-particularly in regard to the mechanism responsible for its origin, subsequent development

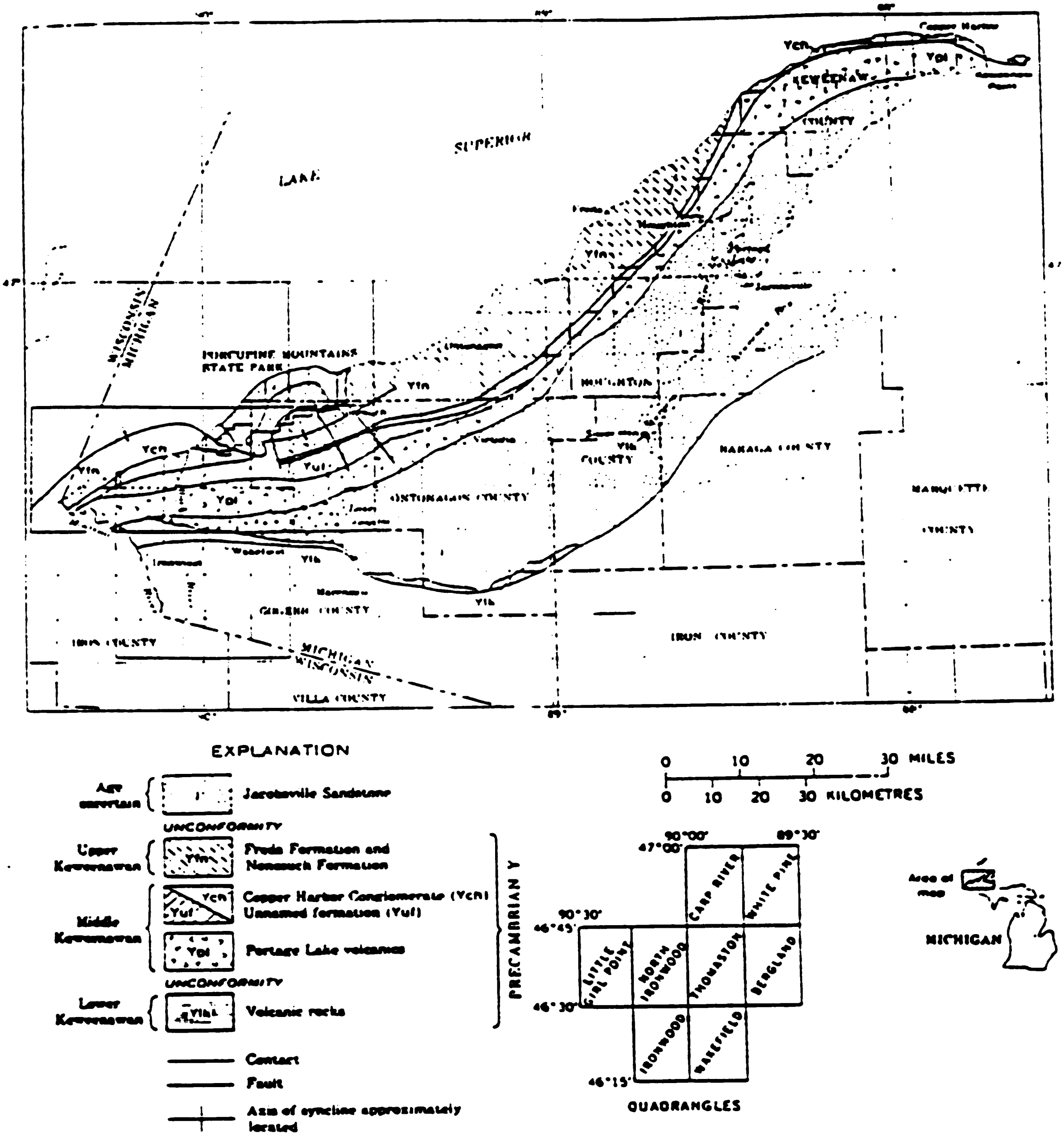

Figure 1
Study Area Location Map

of the rift and basin, and relationship of the rift to contemporaneous tectonism and orogenesis-depend for their answers on new investigative approaches and more detailed studies, particularly of a geochemical and geophysical nature." (pg. 274)

This tectonic activity in the Lake Superior Basin is associated with the Midcontinent Rift system (MCR) of North America (Wold and Hinze 1982) with its pronounced gravity anomaly, hence "the Midcontinent gravity high" (e.g. Chase and Gilmer, 1973). The rift, which extends approximately 2300 km from central Kansas northeastward to Lake Superior through Michigan, constitutes one of the major continental rift systems of the earth.

Exposures of the group of rocks associated with rifting in Michigan provide a nearly complete history of the rift interval, from the development of the quartz arenites of the Bessemer Quartzite which conformably underlie the very earliest volcanic products related to rifting, to the rocks which record the abrupt transition from a volcanic dominated sequence to a period of sedimentation. The early volcanic stages of rifting are represented by the Powder Mill Group (PMG) (Gell, 1988) and the Portage Lake Lavas (PLL) (Paces, 1988). The PMG and PLL are composed primarily of basaltic lava flows. The last volcanic stage of the rifting in Michigan is represented by the mafic to felsic lavas that make up the UF. The UF terminates in the abrupt transition of the volcanic dominated sequence to a period of sedimentation.

The UF is a sequence of subaerially deposited andesite, felsite, and quartz-porphyry rhyolite lava flows interbedded with subordinate sedimentary rocks. Miller (1986) stated that "the origin of great abundances of siliceous volcanic rocks from quartz latites to rhyolite...is unknown and has received little study to date." Kopledowski (1983) and Miller (1986) have however hypothesized as to the origin of the rhyolite bodies associated with the MCR volcanism.

Kopledowski (1983) studied the petrologic and basic geochemistry of the UF and concluded that it is the remnant of a middle Keweenawan central volcano. He divided the mafic lavas into three groups flood basalts, shield basalts, and andesites. He believed that the more evolved lavas were derived by long lived open system fractionation of a magma chamber as described by O'Hara (1977). The compositional variation from basalt to rhyolite was due to a complex volcanic system with multiple vents and magma bodies.

Miller speculates based primarily on the abundance of the silicic magmas that they were not formed by fractional crystallization and instead correlate with his troctolitic stage of wholesale or partial melting of granitic crust.

The purpose of this study is to evaluate petrogenetic models, using standard petrographic techniques, as well as major and trace element variations within the UF, for the evolution of the lavas of the UF, and to test the hypothesis

of Kopledowski (1983) (open system fractionation) vs. that of Miller (1986) (partial melting of crust) for the evolution of the rhyolite flows.

GEOLOGIC SETTING

The extent of the MCR is defined by the Midcontinent Geophysical Anomaly that extends from northeastern Kansas through the Lake Superior Region, and through the Michigan basin. The rocks of the MCR are exposed only in the Lake Superior Region.

The Keweenawan Lake Superior lavas have been recognized as one of the worlds major plateau or flood basalt provinces (Green, 1983). The lava flows are laterally extensive and volumetrically large, up to 400 km^3 (Huber 1973). "As in other continental flood basalt provinces the environment of eruption was one of a broad, flat plain, slowly subsiding, but repeatedly covered by large volumes of fluid...," (Green 1983, pg. 419).

The geology of the UF has been mapped and described by the following U.S.G.S. geologists: Hubbard (1975a) Little Girls Point Quadrangle and North Ironwood Quadrangles; Hubbard (1975b), Carp River and White Pine Quadrangles; Johnson and White (1969), Matchwood Quadrangle; and Whitelow (1974) Rockland and Greenland Quadrangles.

The UF is a sequence of subaerially deposited andesite, felsite, and quartz-porphyry rhyolite lava flows interbedded with subordinate sedimentary rocks. The upper 2,500 feet of the formation forms the knobby upland of the Porcupine Mountains. Regionally, the formation is a volcanic pile which reaches its maximum thickness measurable at the surface of

8,000 feet in the Bergland, and Thomaston quadrangles, about 5 miles south of the Porcupine Mountains. It wedges out in the Greenland quadrangle to the east and the Little Girl Point quadrangle to the west.

The UF is conformable with the underlying Portage Lake Lava Series (PLL) but is distinguishable from it by differences in rock type. The mafic PLL are predominantly basalt, whereas those of the UF are predominantly andesite. The rocks of the UF are finer grained and contain a greater proportion of porphyritic and felsic rocks than do the PLL. The formation was first recognized by Johnson and White (1969) near Oak Bluff in the Matchwood Quadrangle, but they did not name it formally (Hubbard, 1975b).

The formation dips N-NW toward Lake Superior exposing eroded cross sectional views of the flows. The formation is cut by a steeply dipping reverse fault the Keweenawan fault (Figure 2) as well as several minor faults. The outline of the mapped surface of the formation is lensoid, resembling the cross sectional view of a broad central shield volcano (Kopledowski, 1983). Folding has resulted in the finger like projection of the formation in the vicinity of the Porcupine mountains. The cross sectional exposure of the flows makes sampling of successive flows relatively easy in most locations. The folding, faulting and overall poor exposure makes sampling of individual flows along strike difficult at best.

METHODS

The Unnamed Formation outcrops in the western upper peninsula of Michigan in Gogebic Co. and Ontonogan Co.. The aerial extent of the UF is shown on Figure 2 (Hubbard Figure 1 1975). Most outcrops of the formation occur where streams have cut through the mantle of glacial deposits (Hubbard 1975). Exposures of the formation can also be found in the steep slopes, along road cuts, and within quarries.

Sixty three samples of the UF were collected from ten different areas. The sample areas were chosen in order to provide profiles of the formation both across and along strike. The sample areas are located within the North Ironwood, Thomaston, Bergland, and Little Carp Quadrangles.

Each sample was collected from a fresh relatively unmetamorphosed portion of the formation. Where possible consecutive flow centers were sampled in each area. When individual flows could not be identified samples were collected from periodic intervals across strike. Descriptions of each sample location are presented in Appendix A.

Standard petrographic thin sections of the hand samples were prepared in order to determine phenocryst phases and modal percentages present within each sample. This data is used below to help place constraints on the fractionation models. Bulk rock chemistry was determined using X-ray fluorescence for the major oxides and selected trace elements, and instrumental neutron activation analysis (INAA) for

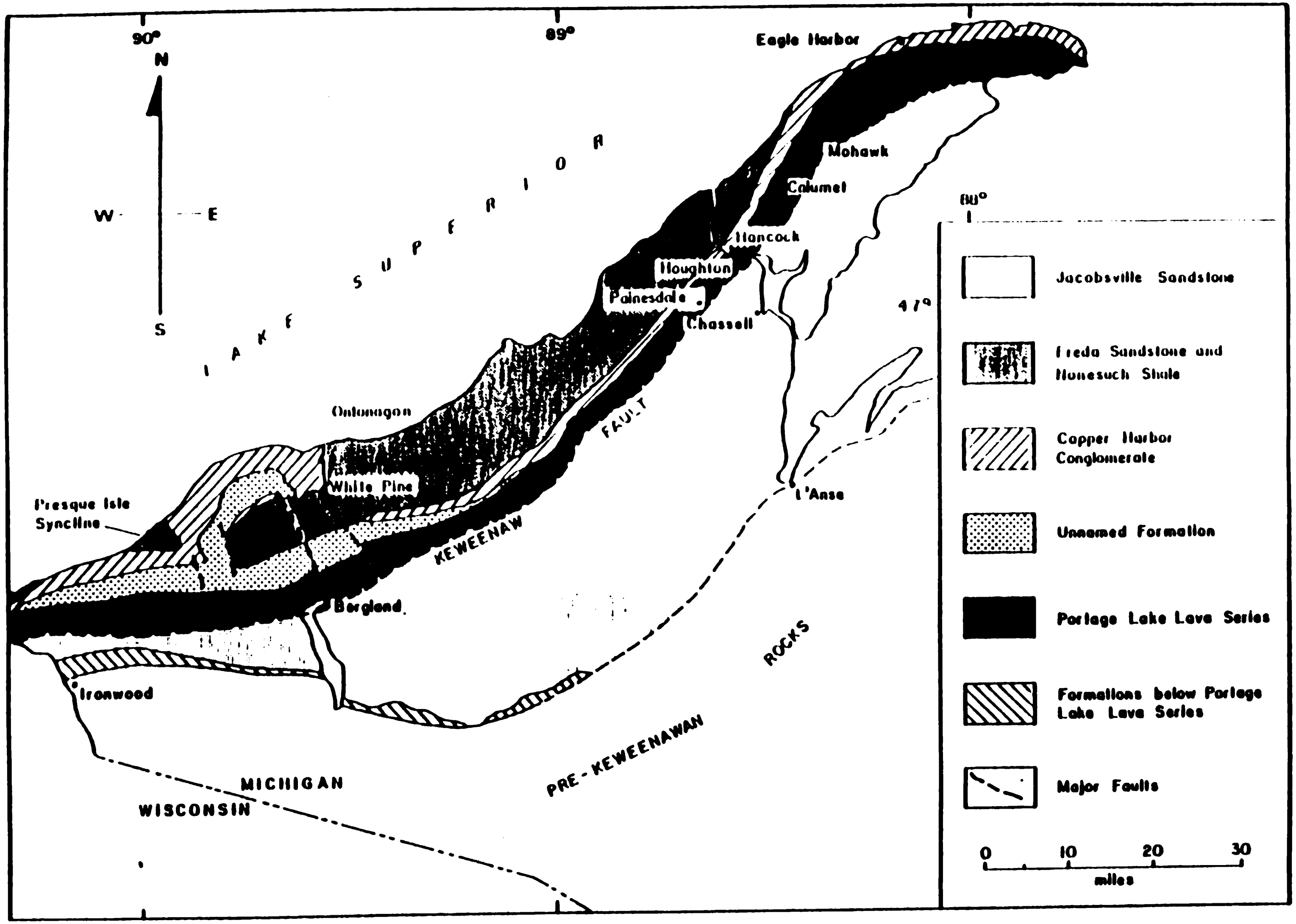

Figure 2
Areal Extent of Unnamed Formation

additional trace elements and selected rare earth elements (REE). Analytical methods and equipment are described in Appendix B. The bulk rock analysis are used along with the methods of Harker (1909), Allegre et.al (1978) Minster et.al (1978), and Pearce (1968) in order to evaluate the fractionation parameters, and to test the hypothesis of Kopledowski (1983) and Miller (1986).

FIELD AND PETROGRAPHIC OBSERVATIONS

The Unnamed Formation is composed of a wide range of rock compositions from mafic to felsic. The mafic rocks are dark colored extrusive rocks of basaltic or andesitic composition. The felsic rocks are light colored extrusive rocks of rhyolitic composition. Andesites and rhyolite are the dominant rock types at the center of the volcanic complex. They are usually exposed on the steep slopes and in quarries. The basalt are dominant on the flanks of the formation. They usually outcrop along rivers and streams.

The mafic rocks range in color from light grey to brown. Unlike the PLL they are usually andesites. Most of the flows are less than 25 ft. (8m) thick and have pahoehoe tops, but some have autobrecciated tops. Flow tops generally contain sparse irregular vesicles filled with chlorite, epidote, quartz and calcite (Hubbard, 1975b). They are fine grained to porphyritic. Plagioclase is generally the dominant mineral phase. Pyroxene, olivine (and/or pseudomorphs), opaque minerals, and minor amounts of amphibole are also present. A summary of the range of modal percentages of minerals determined by thin section is presented in Appendix C. Most of the plagioclase crystals exhibit Albite twinning. The extinction angle of the Albite twins was used to determine the anorthite (An) composition of the plagioclase by the Micheal Levy method. The plagioclase ranged from An 60 (Labradorite) to An 73 (Bytownite). Normal extreme oscillatory zoning of the plagioclase destroyed the usefulness of this technique in many of the samples. The oscillatory zoning is common in rapidly cooled extrusive basalt.

The porphyritic rocks contain phenocrysts of plagioclase and may also contain phenocrysts of pyroxene and/or olivine. The plagioclase phenocrysts occur as well shaped laths. The pyroxene phenocrysts are subhedral and exhibit ophitic texture although subophitic texture is also present. The olivine phenocrysts generally occur as psuedomorphs with the olivine being partially to totally replaced and altered to serpentine and opaque minerals. The matrix of these rocks consists of microcrystalline plagioclase, ferromagnesian minerals and opaques with minor amounts of glass.

The nonporphyritic rocks contain equigranular plagioclase and pyroxene. They are generally trachitic in texture. The subhedral to euhedral plagioclase laths are the dominant mineral phase. Pyroxene, opaques and unidentified alteration products are also present in minor amounts.

The felsic rocks make up approximately 25% of the UF. They range in color from light red to red brown. They are aphanitic to porphyritic. The aphanitic lavas consist primarily of microcrystalline alkali feldspar, plagioclase and quartz. The porphyritic rocks contain phenocrysts of alkali feldspar, plagioclase and quartz that are generally set in a devitrified cryptocrystalline matrix of quartz and feldspar.

The feldspars are usually altered to sericite. Plagioclase can be distinguished from the alkali feldspars by the presence of exsolution perthites in the former. Quartz phenocrysts are either round or embayed with both varieties occurring in some of the samples. The quartz phenocrysts are also cracked in many cases.

An ash-flow tuff was also sampled in section 21 T50N, R41W of the Matchwood NW quadrangle. The tuff contains red brown pumice fragments up to 2 inches in length in a light red to white matrix of cryptocrystalline quartz and feldspar. Minor amounts of small (<2mm) phenocrysts of quartz and feldspar are also present. Ash flow units are commonly associated with silicic volcanism.

GEOCHEMISTRY

Major Element Chemistry

The rocks of the Unnamed Formation have thus far been divided into two diverse groups, mafic and felsic, based on their color and mineral composition. The wide range of rock composition of the UF is also evident in the major oxide chemistry. SiO_2 ranges from 44.25% to 76.91% and MgO from 0.05% to 8.27%. Chemical analysis for all the samples associated with this study are presented in Appendix D. The rocks of the UF appear to span the normal range of compositions from basalt to rhyolite.

In order to relate the variation of the major element data to each other a series of X-Y variation diagrams are presented in Figure 3. Due to the wide range of MgO within the UF, MgO was chosen as the absica with the other major oxides being presented on the ordinate axis. The symbols on the diagrams are referred to as, basalt(o), andesites(*) and rhyolite(Δ) based solely on SiO_2 compositions of <52%;52%-66%;>66% respectively. A great deal of scatter exists in the diagrams, but there appears to be two populations, the basalts and rhyolites, while some basalts and the andesites appear to be transitional between the two populations.

Scatter in X-Y plots, such as those presented on Figure 3, is often observed within phenocryst rich lavas (Cross et. al. 1903). The CIPW norms for the UF samples are presented in Appendix E and show that the rocks of the UF are silica

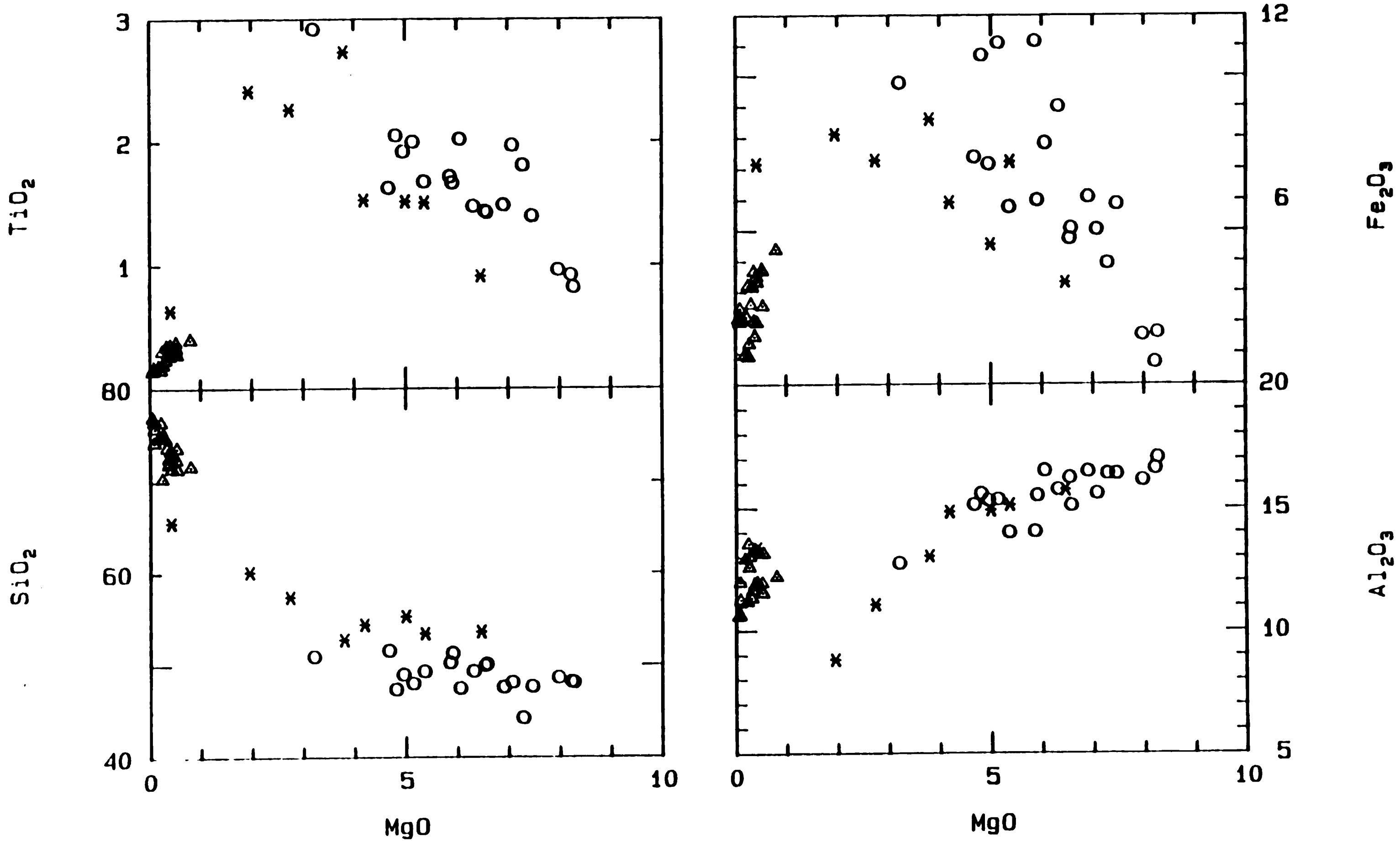

Figure 3
Major Element X-Y Variation Diagrams

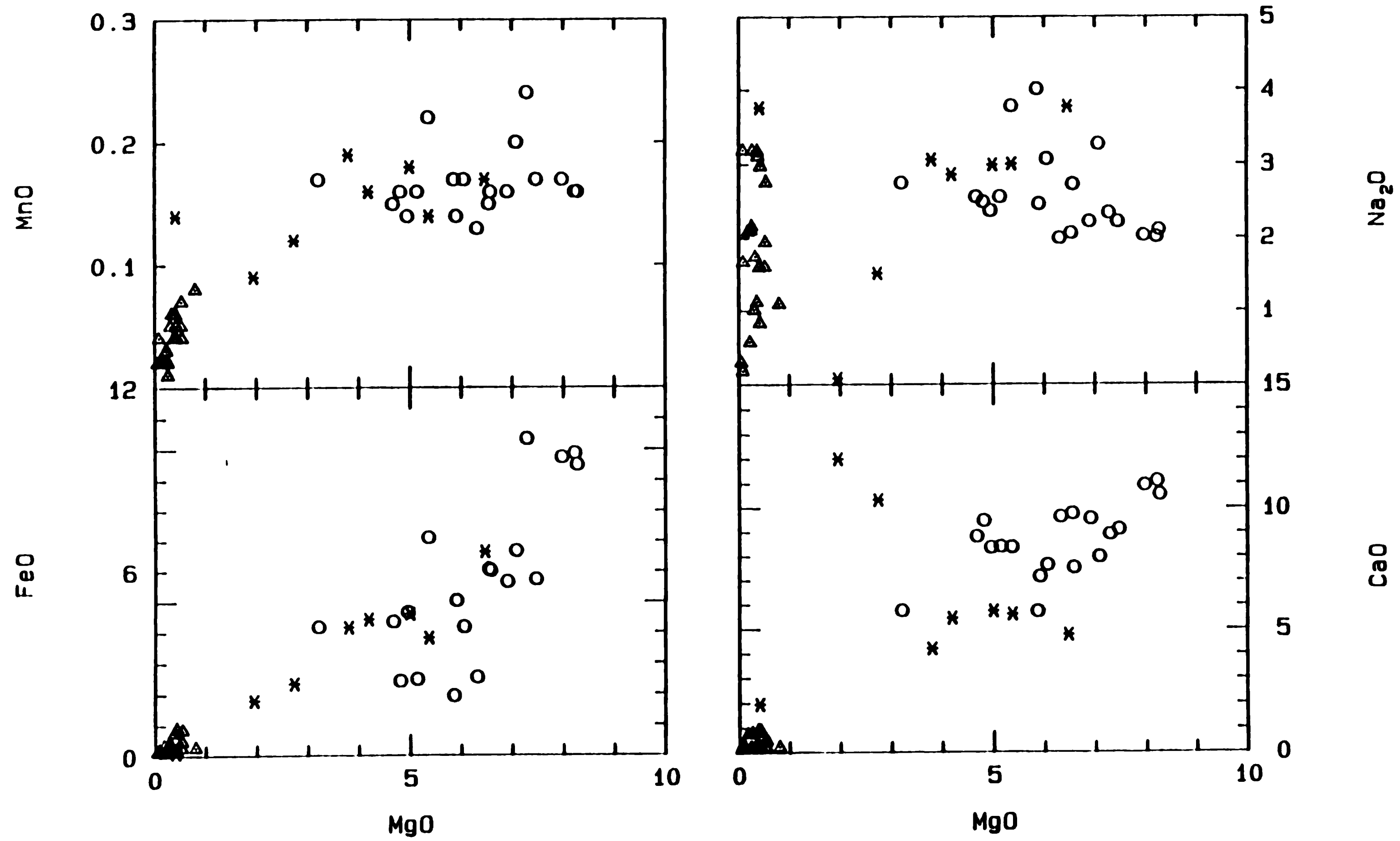

Figure 3
(Continued)

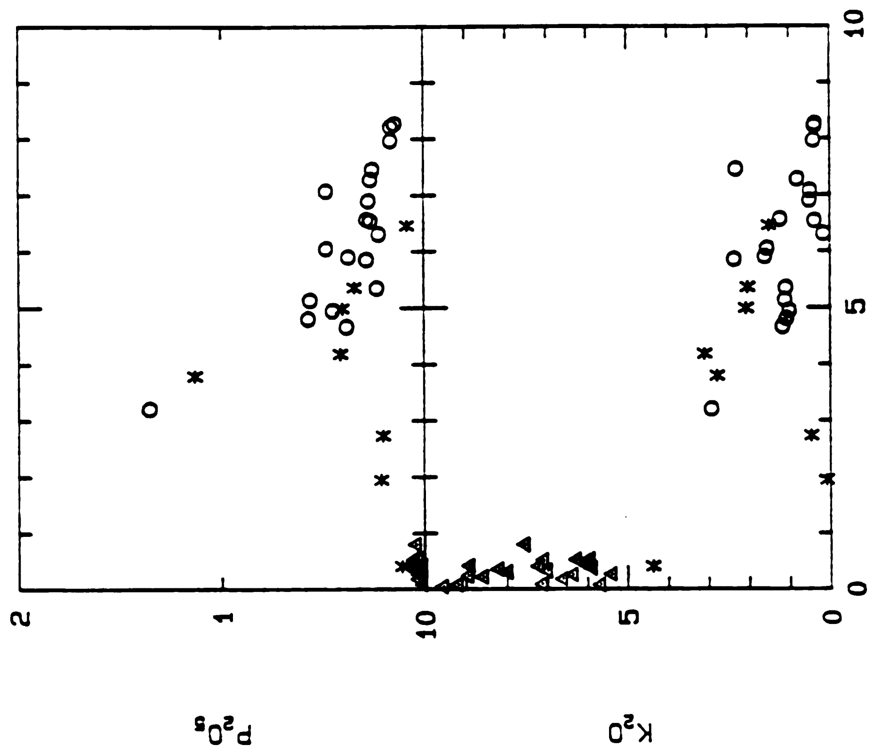

Figure 3
(Continued)

saturated to silica oversaturated. Irving and Baragar (1975) used the CIPW norm in presenting a classification scheme for common volcanic rocks. The AFM diagram on Figure 4 shows that the rocks of the UF are calc-alkaline to tholeitic. A slight iron enrichment trend is evident within the tholeitic basalts of the formation.

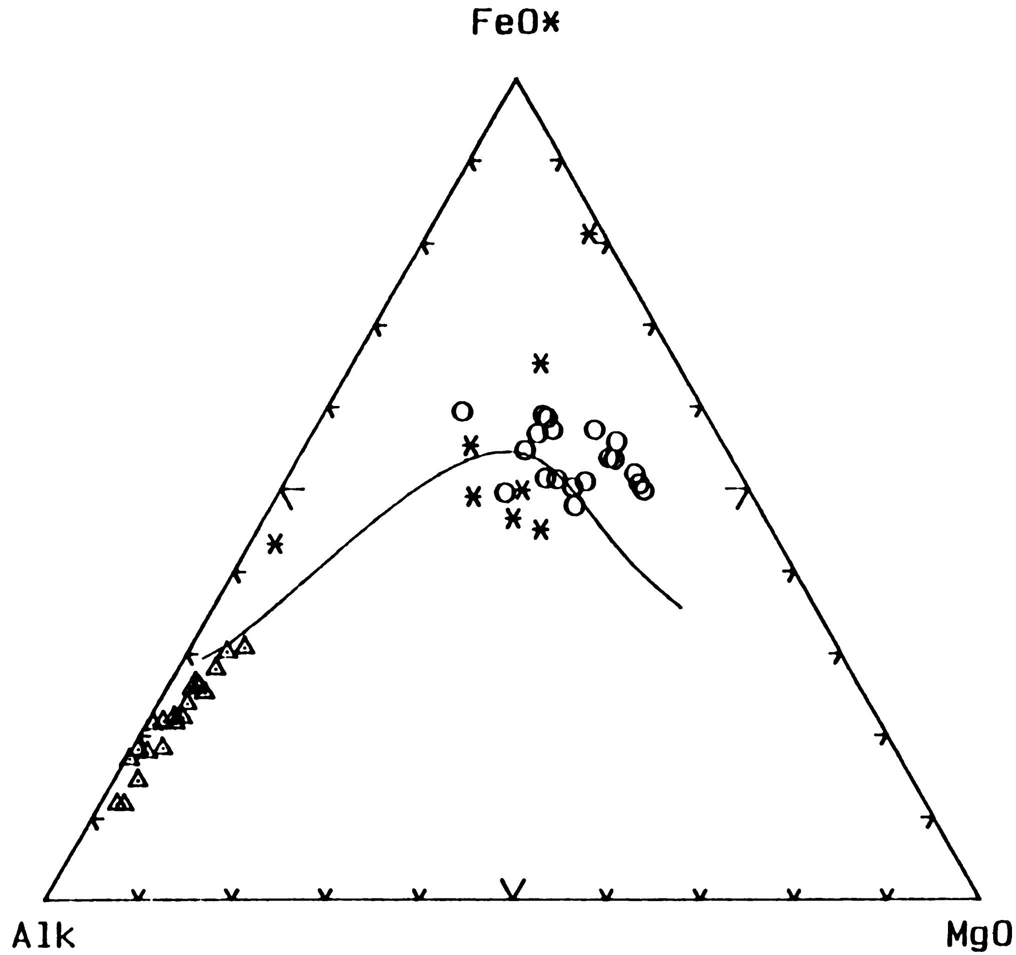

Figure 4
AFM Diagram

Trace Element and Rare Earth Element Chemistry

The trace elements examined in this study are Ni, Cu, Zn, Sr, Rb, Y, Zr, Nb, Ba, Cr, Hf, Th and the rare earth elements La, Ce, Sm, Eu, Tb, Yb, and Lu.

Major element geochemical variations are governed by the stoichiometry and phase relationships of the melt. Their concentrations are also subject to the statistical element of closure. Trace elements are considered to be dilute components of both the solid and liquid phases. Because dilute solutions are not controlled by the same physical and chemical constraints which apply to the essential constituents (Hanson and Langmuir 1978) and they are not subject to the statistical elements of closure, trace element variation can provide independent criteria for the analysis of petrogenetic models.

The trace element data is presented along with the major element data in Appendix D. As with the major element data it is important to plot the data on some sort of variation diagram so that any trends or patterns become more obvious. Selected trace element data is presented on X-Y plots with MgO as the abscissa in Figure 5. The symbols on the diagrams are the same as presented in Figure 3. As with the major oxide data a great deal of scatter exists. The basalt and rhyolite show two different populations, with some basalts and the andesites transitional between the two populations.

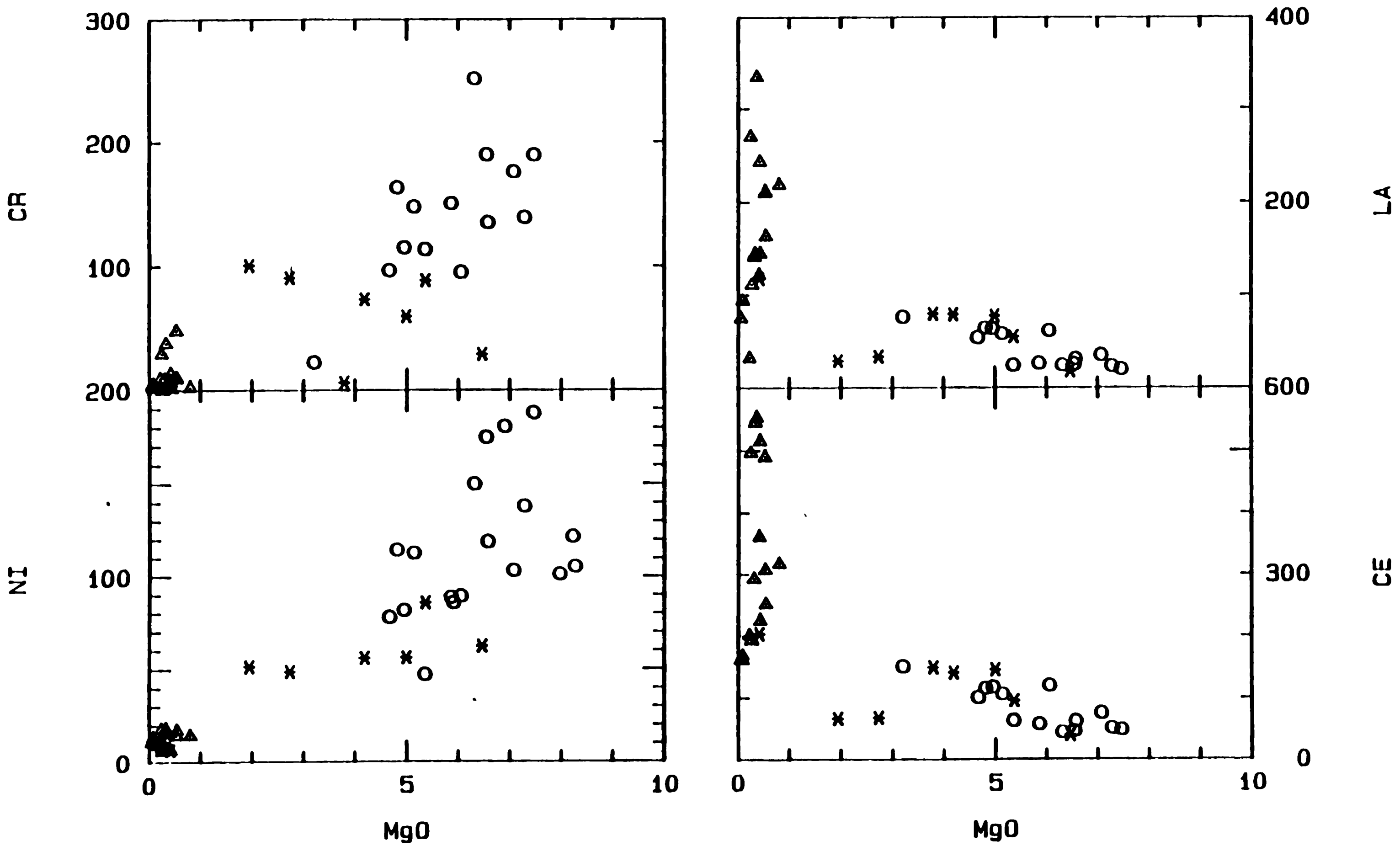

Figure 5
Trace Element X-Y Variation Diagrams

The use of trace element ratios rather than absolute values is important. Ratios make it possible to eliminate the influence of heterogeneous source concentrations, and examine relative trace element behavior. It has been shown that within evolutionally related rocks trace elements behave in a predictable manner (Allegre et. al 1978). Assessment of the relationship of various trace elements in a suite of rocks can lead to constraints on the evolutionary process(es) that lead to their formation.

A commonly used relationship is that of chondrite normalized rare earth elements ($REE_{C}H$). Partial melting of a source will enrich the liquid in the light rare earth elements (LREE) relative to the heavy rare earth elements (HREE). Conversely, the original source will be depleted in the LREE relative to the HREE. The assessment of REE data leads to constraints on the source composition.

Plots of the chondrite normalized rare earth element (REE) data of the UF are presented on Figure 6a. Figures 6b to 6d show the basalt, andesite and rhyolite data respectively. The REE data spans the range from 50 to 1,000 times chondrite, La and from 9 to 40 times chondrite, Yb. The $LREE_{CH}$ ratio increases more than the $HREE_{CH}$ ratio with La/Yb ratios ranging from 4.40 to 39.81.

The basaltic rocks have REE patterns that are approximately linear with low slopes and no Eu anomaly. The andesite $REE_{C}H$ data also exhibits an approximate linear

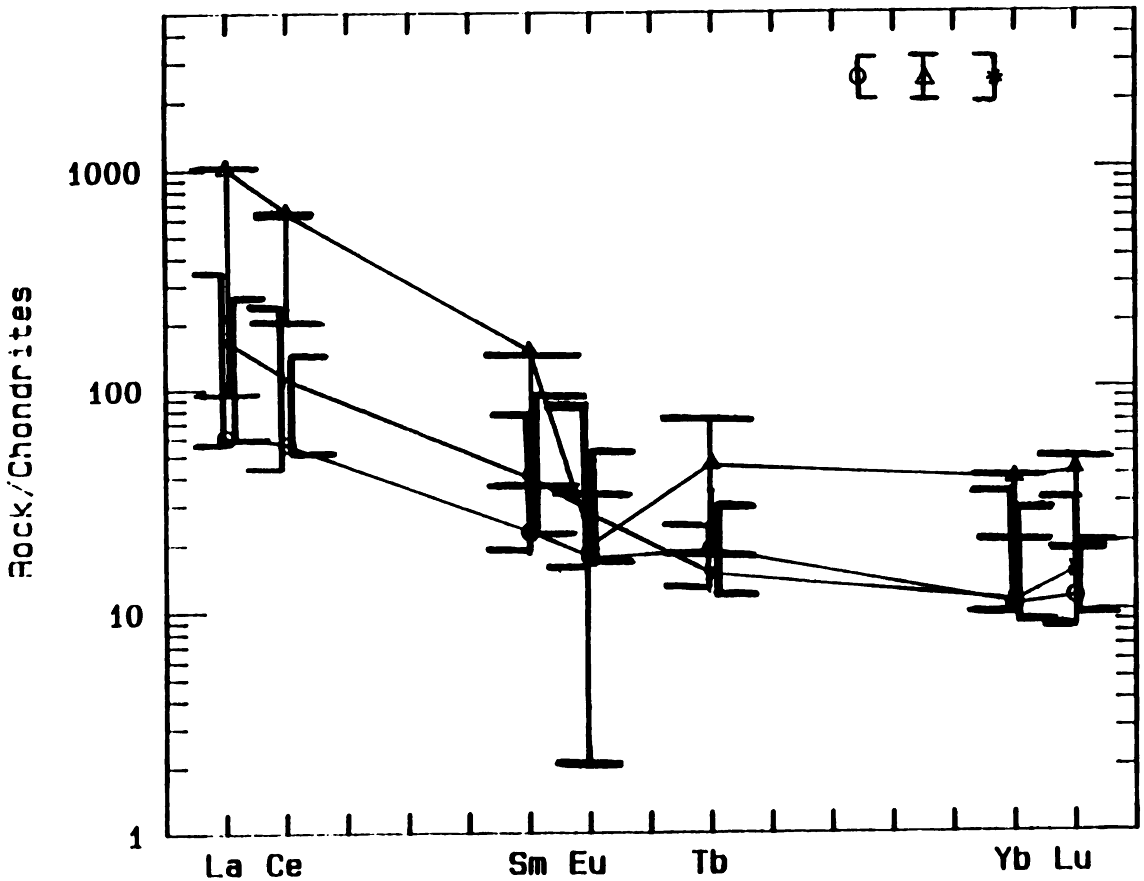

Figure 6a
REE Plots: Ranges

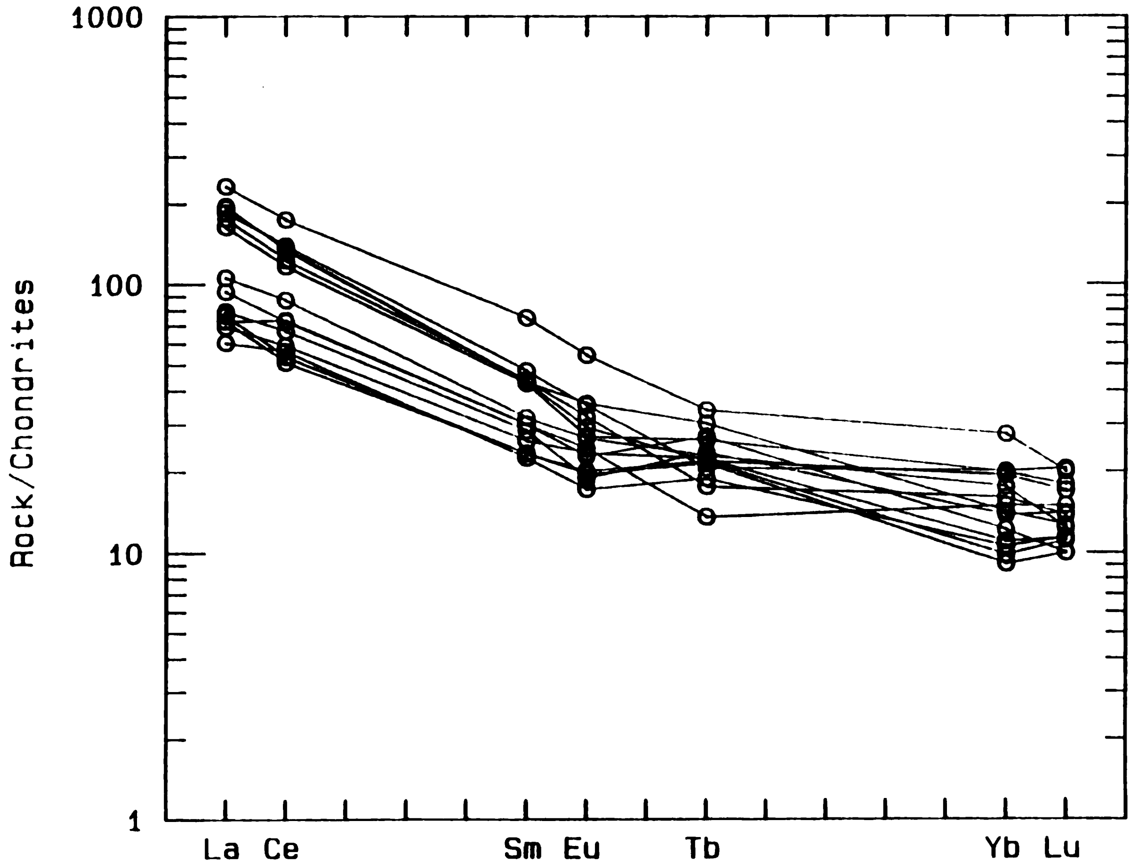

Figure 6b
REE Plots: Basalts

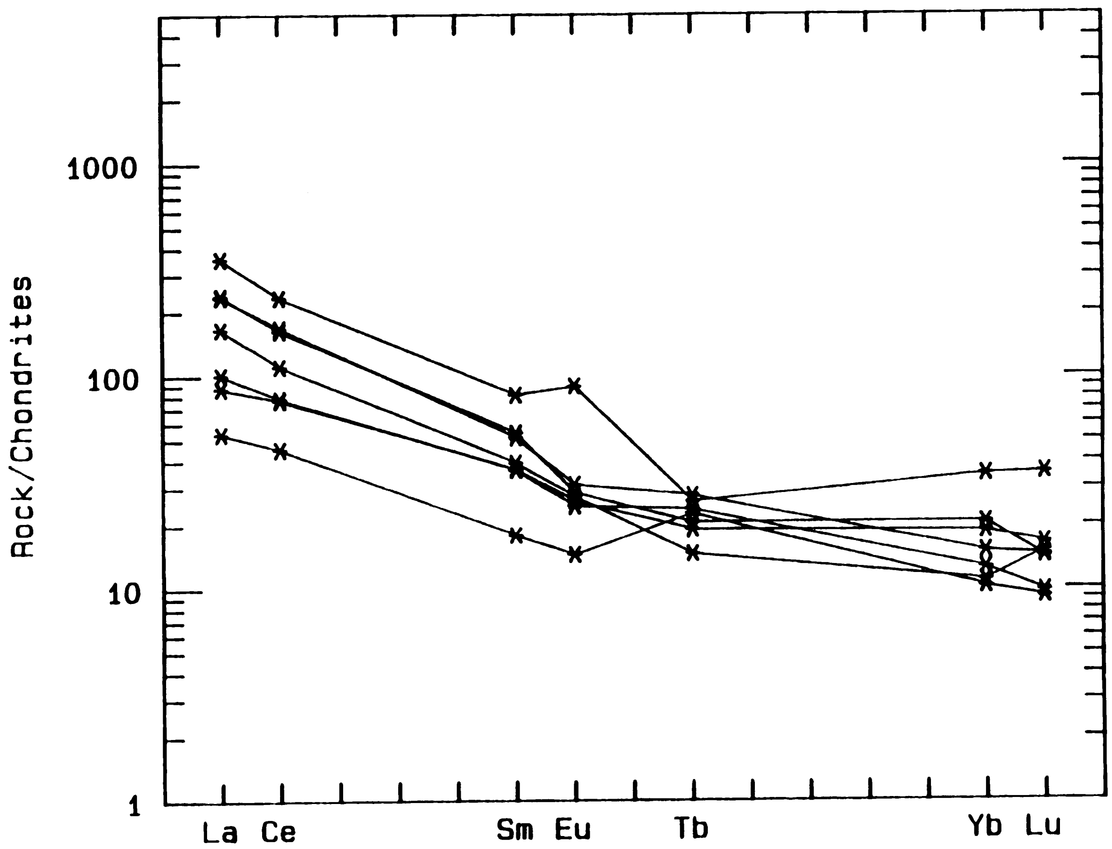

Figure 6c
REE Plots: Andesites

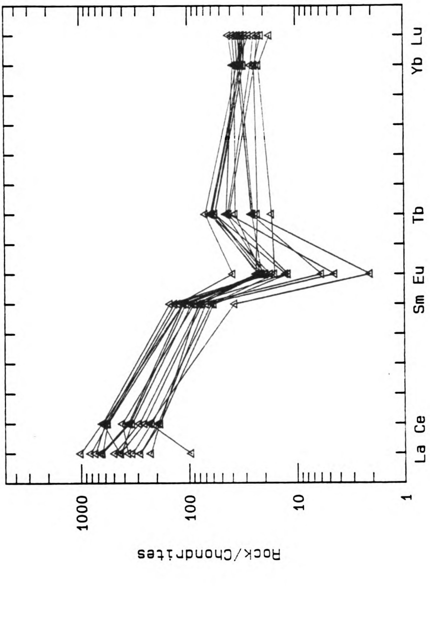

Figure 6d
REE Plots: Ryholites

pattern with a greater slope than the basalts. A slight Eu anomaly appears within the andesites and sample TQ-5 shows a positive Eu anomaly. The rhyolite REE patterns have steeper slopes than the andesite data and include a pronounced Eu anomaly. The Eu anomaly is more pronounced for lower $LREE_{CH}$ values.

QUALITATIVE ANALYSIS OF DATA

Allegre and Minster (1978) and Minster and Allegre (1978) have presented graphical methods for identifying the process(es) involved in the evolution of a rock series by the use of qualitative characters of trace element behaviors. Three categories of elements are considered to distinguish between the main processes (a) Elements of high solid-liquid partition coefficients e.g. Ni or Cr: these elements vary drastically in successive liquids during fractional crystallization, the concentrations of such elements in lava derived by partial melting are insensitive to the degrees of melting. (b) Elements of low partition coefficients: these elements have been called hygromagmatophile elements by Treuil (1973) or H elements by Allegre et. al. (1977). Their bulk partition coefficients can be approximated to be 0. In fractional crystallization or partial melting processes, the concentration of such an element in the liquid is inversely proportional to F, the percent liquid remaining. As a consequence its abundance is far greater in the case of melting processes. (c) Elements of intermediate partition coefficients: in the case of partial melting the bulk partition coefficient should be compared with the degree of melting (F) because when the degree of melting is low two elements with intermediate partition coefficients (i.e. negligible against 1, but not against F, e.g. D=0.1) may not yield constant concentration ratio in the liquid. The variation of such ratios is larger for fractional melting than for batch partial melting. It is negligible during fractional crystallization.

A series of the process identification diagrams (Allegre and Minster, 1978 and Minster and Allegre, 1978) is presented in Figure 7. These diagrams use incompatible trace elements and ratios of incompatible trace elements to assess the variation within a rock suite. The clustered data of the basalts and andesites indicates that they may have been formed through fractional crystallization processes. As a magma crystallizes the incompatible elements would be preferentially excluded from the crystallizing minerals. This would increase their overall abundance, but their ratios will remain constant until large degrees of crystallization have occured.

The rhyolite data has distinct non horizontal linear trends that indicate they were formed due to melting processes. As a source rock is melted the incompatible trace elements are preferentially incorporated in the liquid. This, coupled with various degrees of melting (F) leads to a wide variation in their abundance in the resultant magma. The slight differences in incompatible trace element bulk distribution coefficients also leads to changes in the ratios between two incompatible elements. These slightly differing D's and the wide variation within each incompatible trace element lead to the non horizontal linear trends on the incompatible element process identification diagrams.

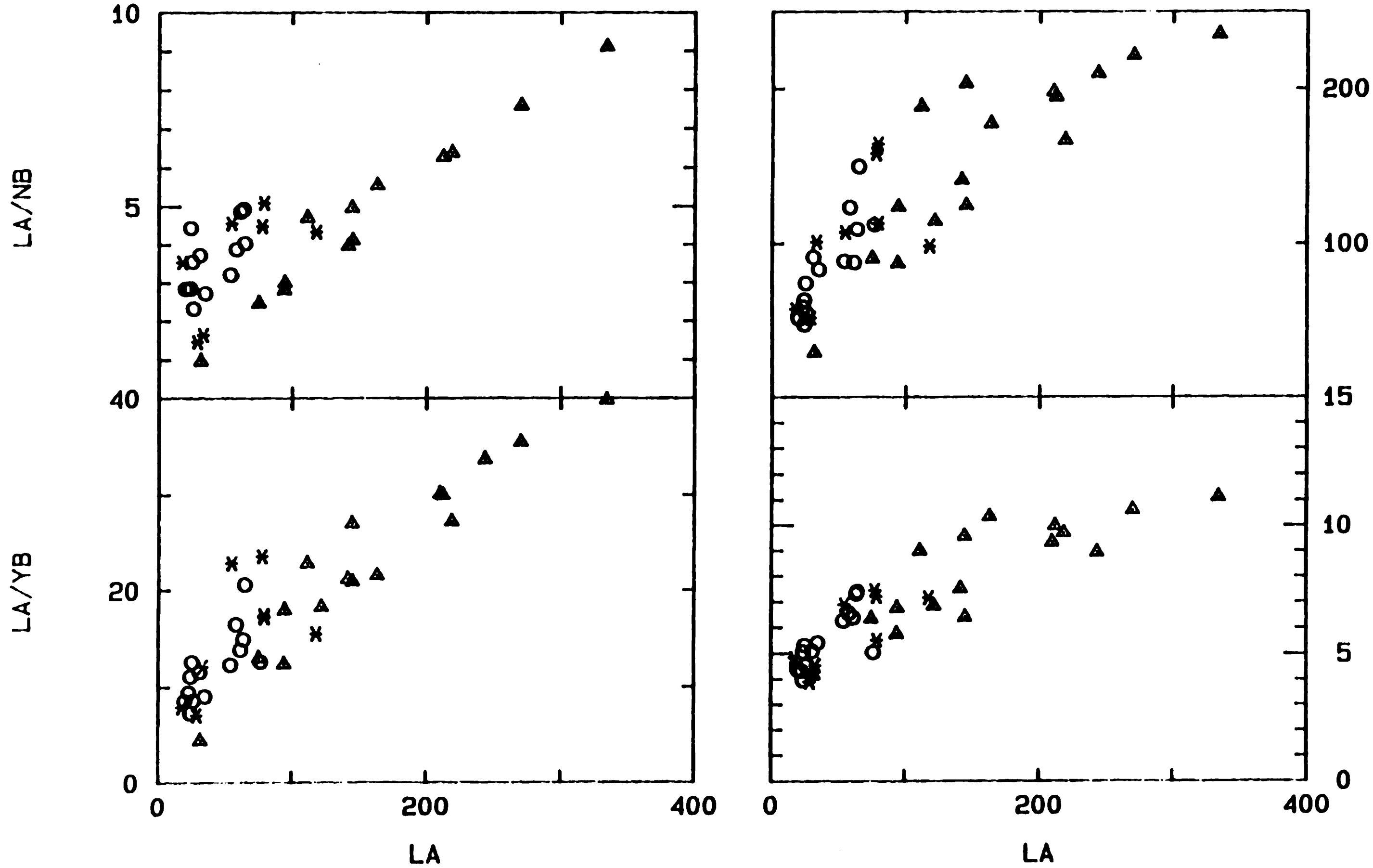

Figure 7
Process Identification Diagrams

QUANTITATIVE ANALYSIS OF DATA

Basalts and Andesites

As stated earlier the major element data is subject to the statistical elements of closure. Stanley and Russell (1988) have developed a computer program to analyze rock compositions based on Pearce element ratio diagrams (Pearce, 1968). Pearce recognized that if at least one conserved element is present within a suite of rocks the analytical data can be used to determine the exact relationship between the non-conserved elements. The conserved element is used as the denominator in ratios of non-conserved elements in order to assess the relationship between the non-conserved elements. In essence the data are normalized to the conserved element and this eliminates the closure problem.

Pearce element ratios can also be used to distinguish comagmatic lavas. Figure 8a shows Pearce element ratios of Ti/K vs. P/K to test a comagmatic hypothesis for all of the lavas of the unnamed formation. Comagmatic lavas on this diagram should form a cluster or the elements are not conserved. As can be seen from Figure 8a, the basalts and rhyolites do not form a single cluster. The basalts as a group however, do form a single cluster and are therefore comagmatic.

A series of Pearce element ratio diagrams were prepared, using only the basalt and andesite data, that assess various crystallizing phase assemblages. Figure 8b represents

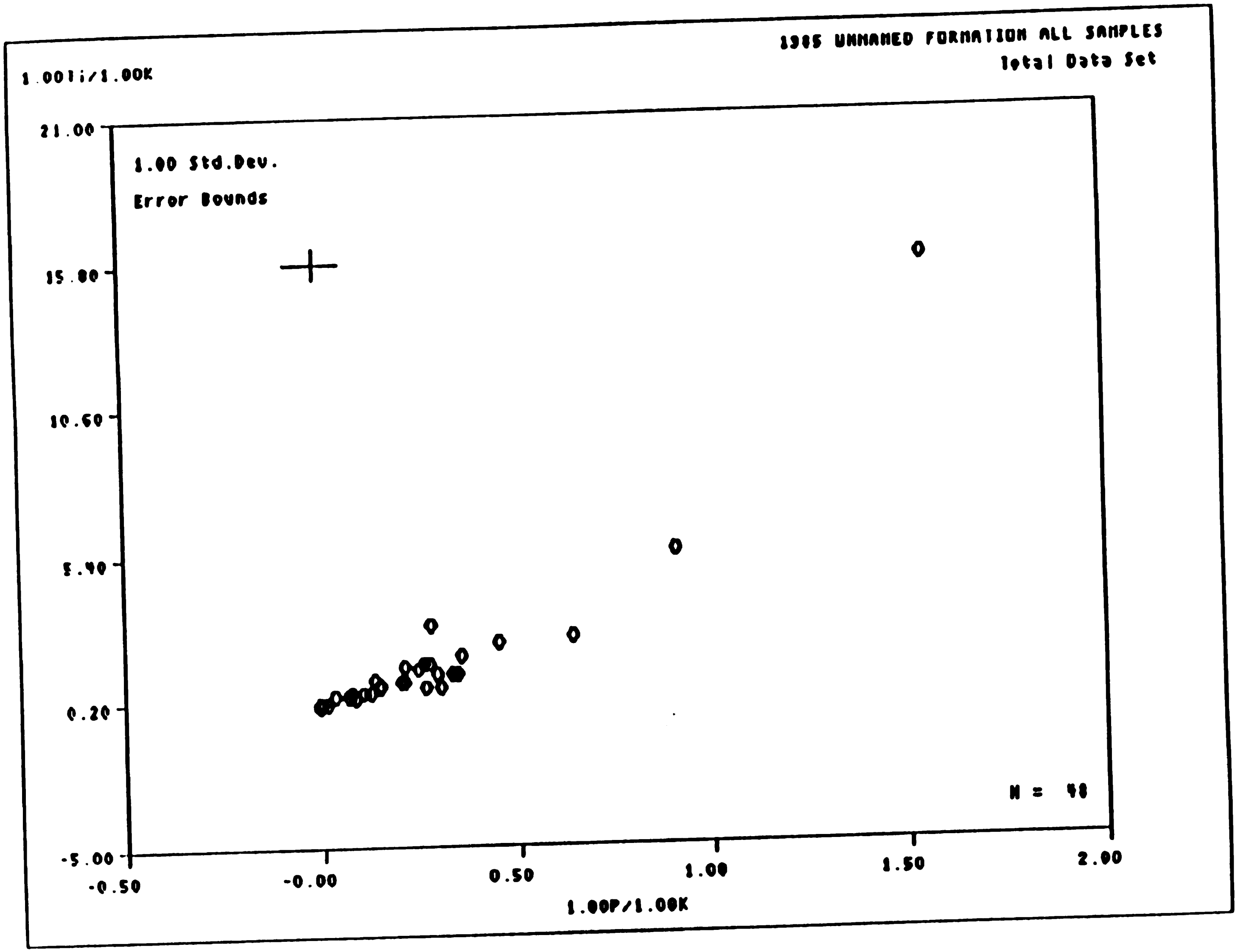

Figure 8a
Pearce Element Ratio Diagram: Conserved Elements

crystallization olivine and augite and Figure 8c represents crystallization of olivine, augite, and plagioclase. Each diagram was constructed so that fractionation of the above mentioned phases would define a slope with a trend of one.

From Figures 8b&c it can be seen that the basalts and andesites were derived primarily from fractional crystallization of olivine, plagioclase, and augite. The slope of the line on Figure 8c is 0.92 with an R^2 of 0.99 as opposed to Figure 8b, 0.53 and 0.97, respectively. Clearly the majority of the variance within this suite of rocks can be accounted for through fractionation of these phases. There is however something else that accounts for the rest of the variation.

Through least squares analysis using a primitive basalt (NIQ-2, Ni=188ppm) as the parent and an evolved andesite (LC-2, Ni=85.80) as the daughter it was determined that the relative proportions of olivine, plagioclase, and augite were on the order of 26:54:20. The least squares analysis is presented in Appendix F. Sum of squares residuals were relatively good (0.578), but there were still other factors involved. The high residuals that were calculated for the compatible element Cr led to the assumption that spinel was also a fractionating phase.

The bulk distribution coefficients listed in Appendix G were taken from Miller (1986) and assigned to the trace elements as an independent test of the fractionation scenario.

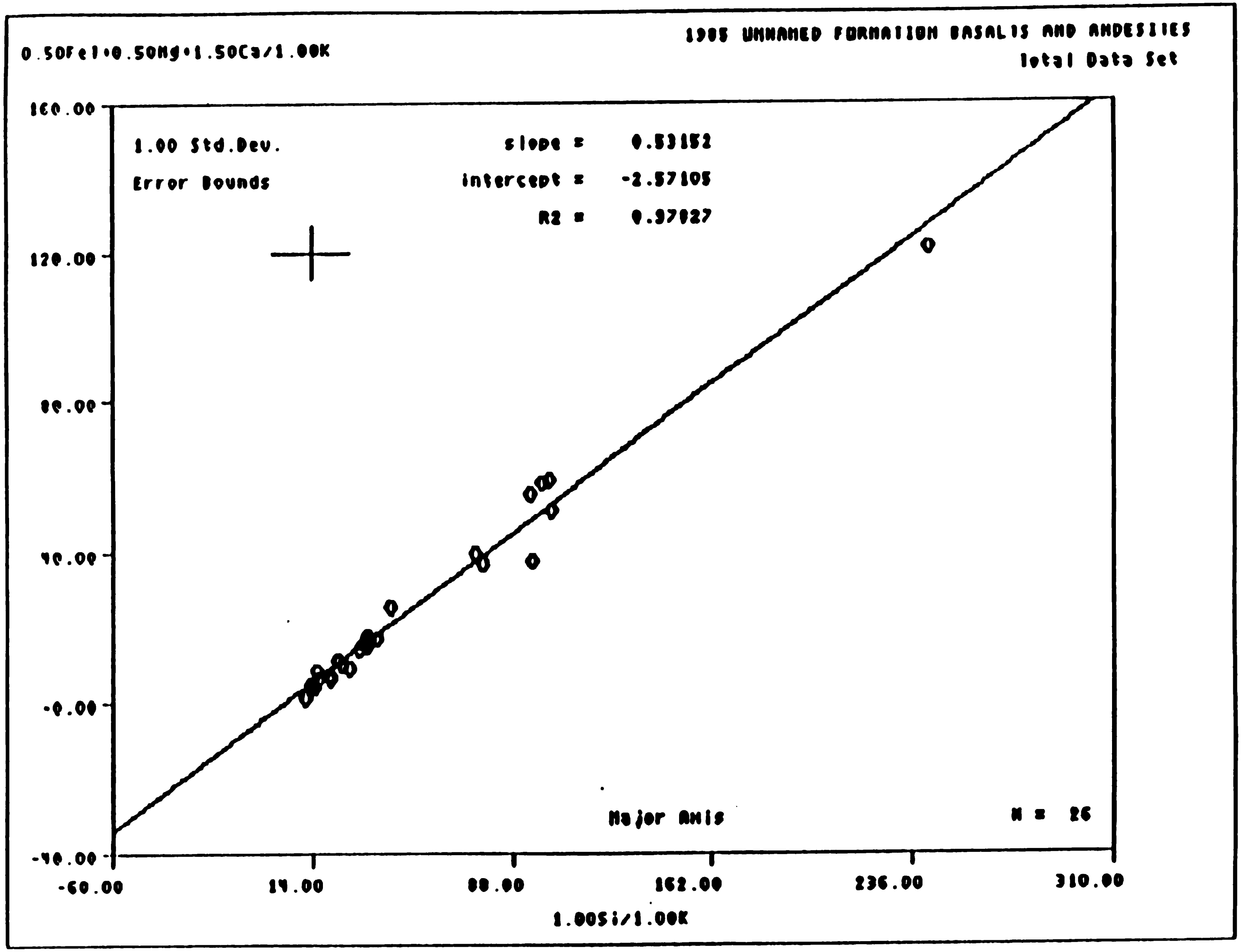

Figure 8b
Pearce Element Ratio Diagram: Olivine + Augite

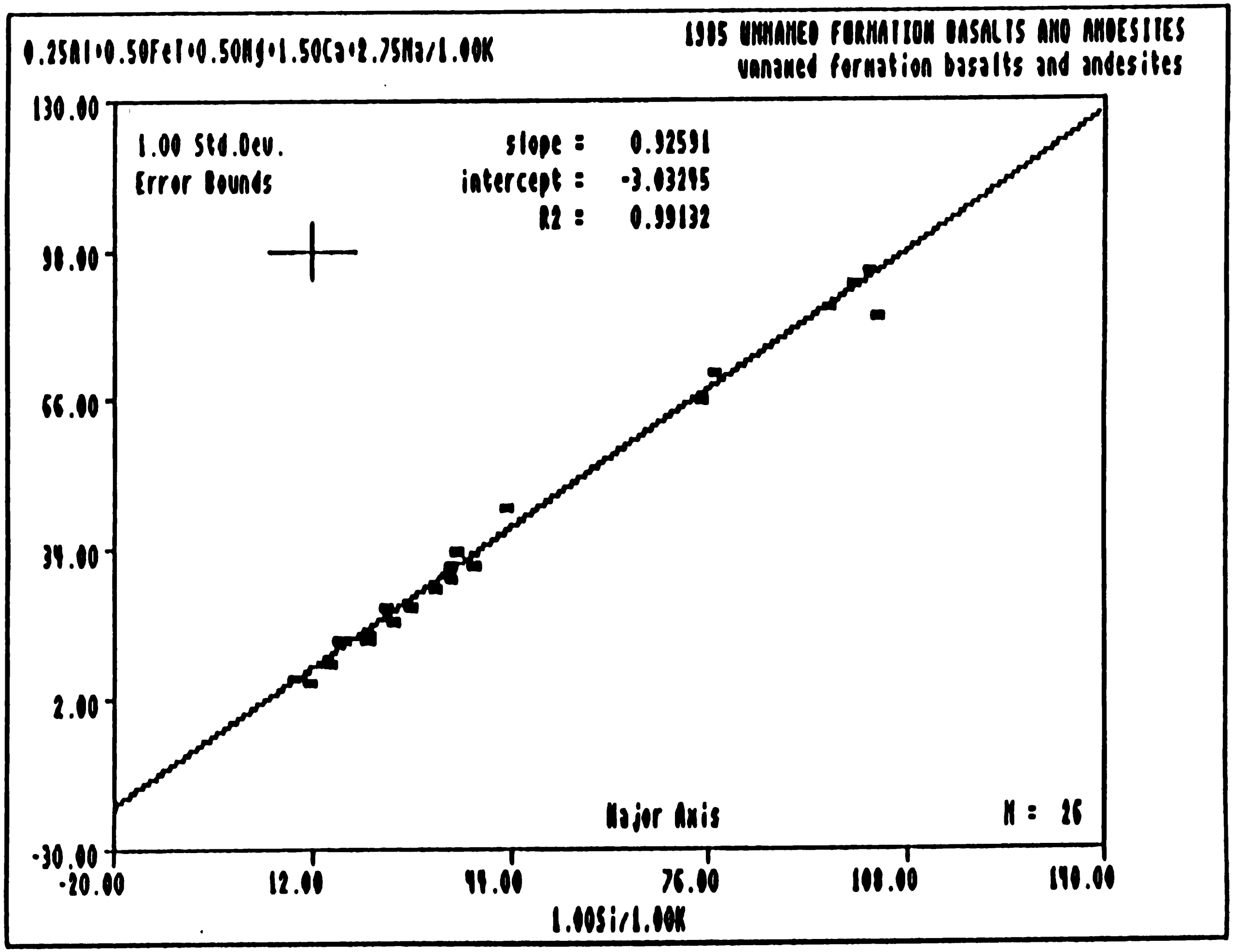

Figure 8c
Pearce Element Ratio Diagram: Olivine + Augite + Plagioclase

Figure 9a shows the results of 10,20 and 30% fractionation of plagioclase(53%), augite(20%), olivine(25-27%)and spinel(0-2%) from an original liquid of composition similar to NIQ-2 with respect to two compatible elements (Ni vs. Cr). The symbols on the diagram represent the basalts and andesite data as previously described. The theoretical fractionation trends are represented by ⊡, △, and □ with spinel varying from 0-2% respectively and olivine varying accordingly. It can be seen from this diagram that the compatible element diversity can be accounted for by up to 30% fractional crystallization of olivine, plagioclase, and augite ± spinel from an original composition like NIQ-2.

A plot of two incompatible elements (La vs. Ce) for the basalts and andesites is shown in Figure 9b. The basalt and andesite symbols are as previously described. The theoretical fractionation of up to 30% of NIQ-2 is represented by the △. It can be seen from this diagram that the diversity in the incompatible trace elements can not be accounted for by the same fractionation scenario that accounts for the diversity in the compatible trace elements.

Because the basalts and rhyolites are spatially and temporally related, magma mixing may have occurred between the two magmas. Again using the composition of NIQ-2 as the parent it was theoretically mixed with up to 50% of an evolved rhyolite (MNW-1). The La vs. Ce plot shown on Figure 10 contains the basalt and andesite data as well as the

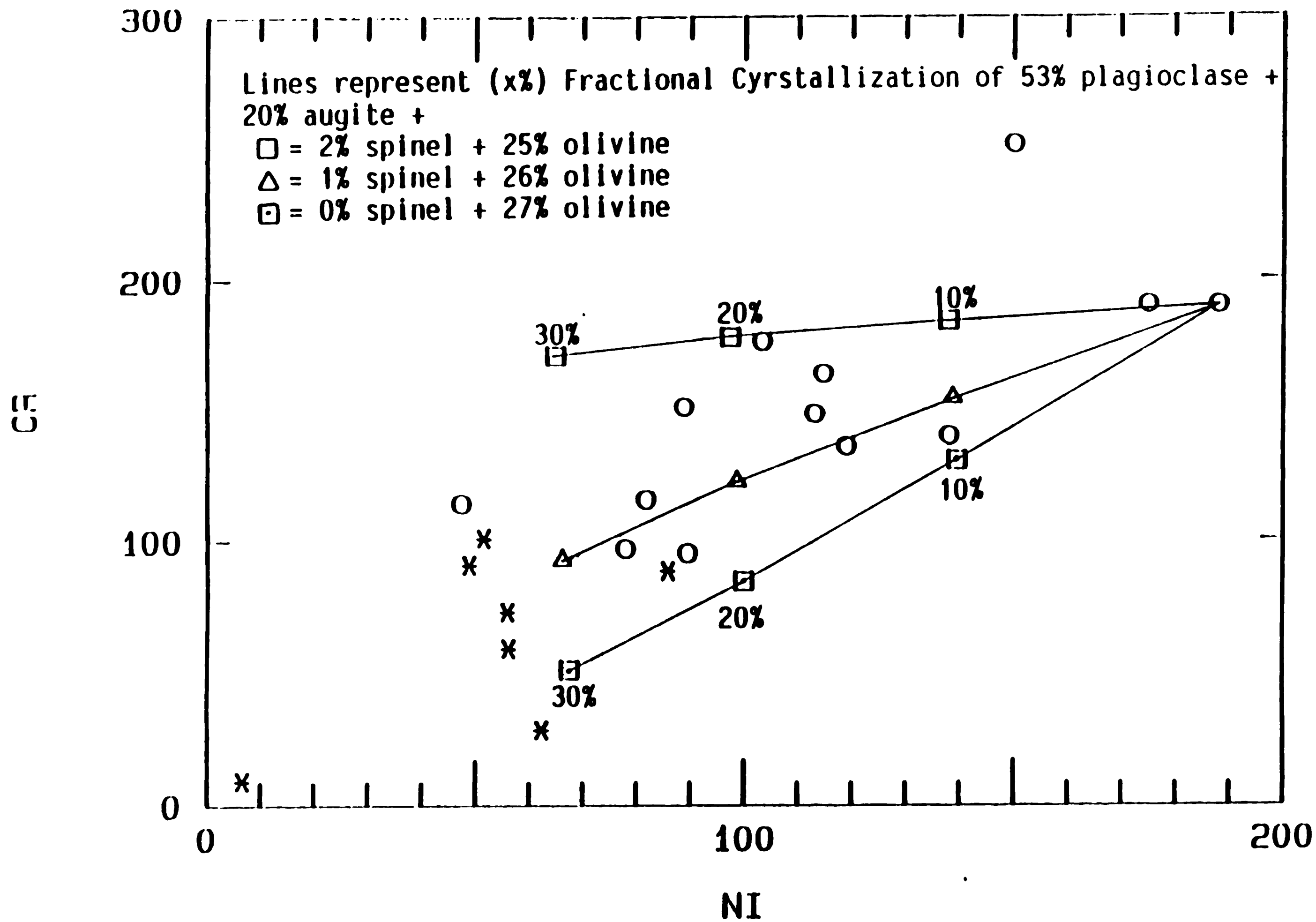

Figure 9a
Theoretical Fractional Crystallization: Compatible Elements

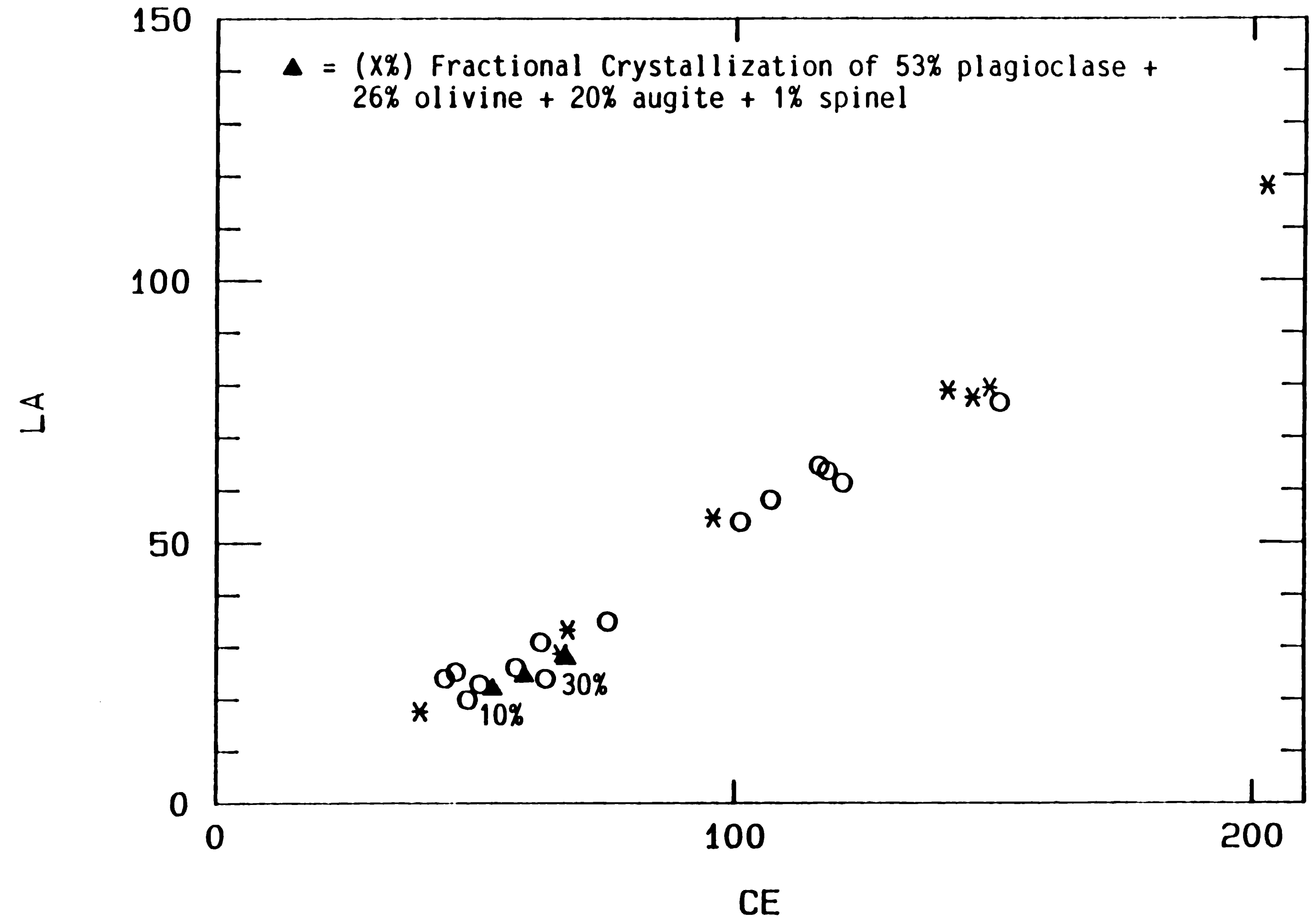

Figure 9b
Theoretical Fractional Crystallization: Incompatable Elements

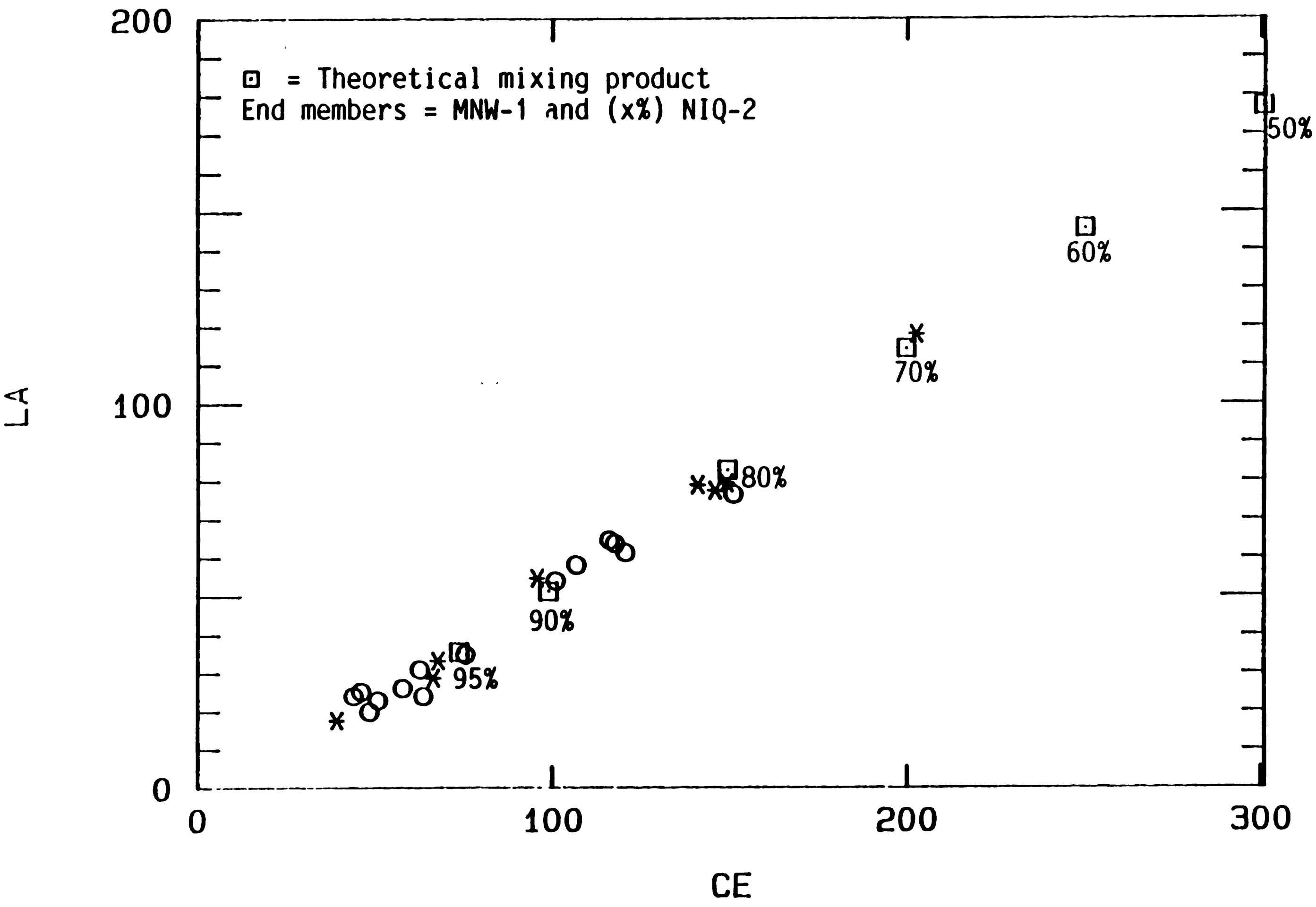

Figure 10
Theoretical Magma Mixing

theoretical mixing derivatives ($\boxed{\cdot}$). The diversity in the trace elements within the basalts and andesites can be derived by mixing of up to 30% of an evolved source (MNW-1) with a primitive parent (NIQ-2).

Appendix F also contains an example of a least squares regression analysis of NIQ-2 with the addition of MNW-1 as well as the subtraction of the fractionating phases. As can be seen from the example, this effort was less successful at achieving a good match with a particular daughter product. This does not preclude the magma mixing hypothesis since the incompatible trace elements would be much more mobile within a partial melt and are thus more sensitive indicators of this process.

It is concluded from the above information that the diversity within the basalts and andesites is consistent with fractional crystallization as indicated through the Pearce plots but that the fractional crystallization must have been accompanied by magma mixing with an evolved source to account for the trace element distributions.

Rhyolites

The process identification diagrams (Figure 7) indicate that the rhyolites of the UF were formed due to varying degrees of partial melting. An equilibrium batch partial melting model was used to model the effects of varying degrees of partial melting on a likely source rock. LC-2, an average andesite, was chosen as the source.

As with the fractional crystallization data theoretical products were plotted on a variation diagram (Figure 11a&b). The □'s represent 1%,10%,20%, and 30% partial melting of LC-2 with mineral percentages of 25:20:55; olivine, augite and plagioclase, as determined earlier and melting percentages of 14:52:34 after Miller, 1986. It can be seen from Figure 11a&b that the majority of the variation within the rhyolites may be accounted for by partial melting of this source. The rhyolites that fall above the main linear trend on the Ce vs. La plot (Figure 11b) show, however that not all the data is consistent with partial melting of a single source. This may be the result of the rhyolites being formed from more than one source location or could be indicative of magma mixing. Further efforts to quantify the degree of magma mixing and extent of partial melting were unsuccessful due to the complexity of the multi-source, multi-mixing components regime.

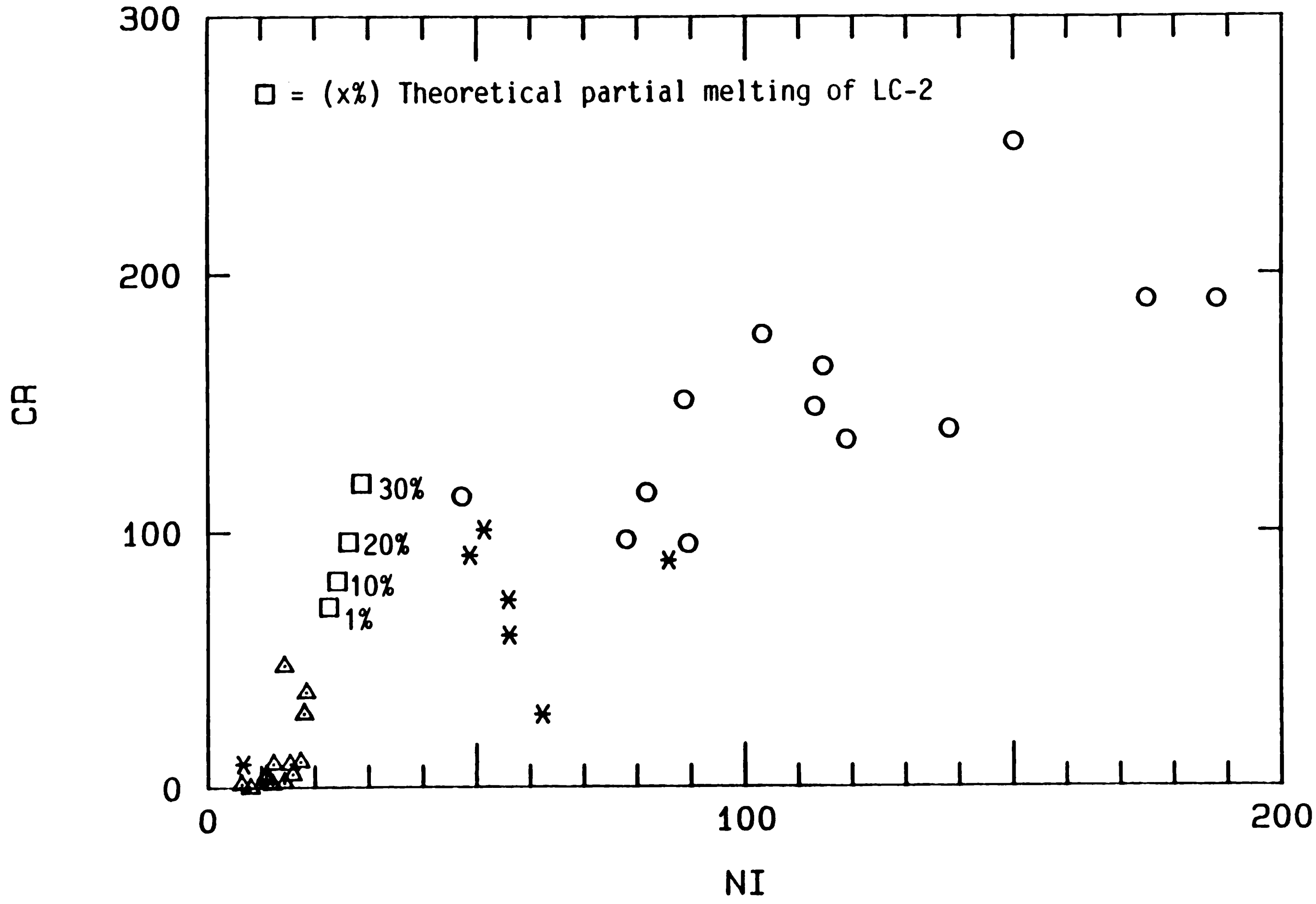

Figure 11a
Theoretical Partial Melting: Compatible Elements

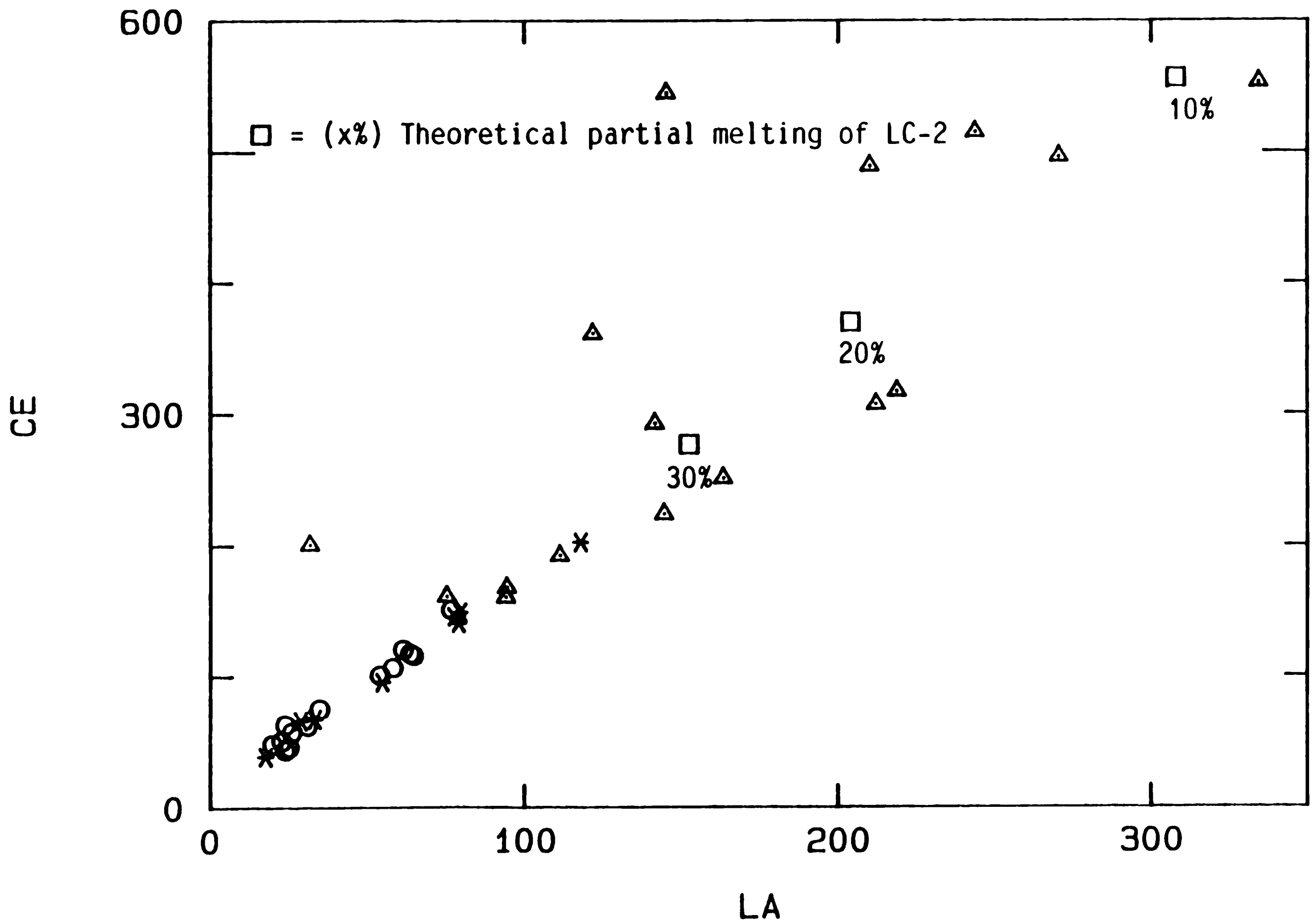

Figure 11b
Theoretical Partial Melting: Incompatible Elements

METAMORPHISM

Jolly and Smith (1972) concluded that the Portage Lake Volcanics were subjected to low rank metamorphism of the zeolite and prehnite-pumpellyite facies. Scofield (1976) described this metamorphism as resulting from geothermal fluids ascending along permeable zones in the flow tops and conglomerates. Kopledowski (1983) concluded that the rhyolites of the Unnamed Formation underwent some type of potassic alteration were the rocks were relatively enriched in potassium and depleted in sodium. As discussed in earlier sections the UF does exhibit signs of low rank metamorphism.

Potassium was used as the conserved element in the Pearce element ratio diagrams which were the basis for the fractional crystallization scenario. Inorder to assess the importance of the potassic metasomatism a plot of Rb vs. Rb/Sr (Hammond, 1986) was used because of the similarity in geochemical behavior between Rb and K. This plot is presented on Figure 12. The non-horizontal linear trend within the basalts and andesites is indicative of plagioclase fractionation. The rhyolites that fall to the right of this line indicate that Rb (and thus K) has been added to the system.

The trace element distributions used to provide evidence of melting processes could also have arisen do to this potassic metasomatism. If the metasomatism has given rise to the trace element distribution then the trace element distribution should be correlated with some indicator of the

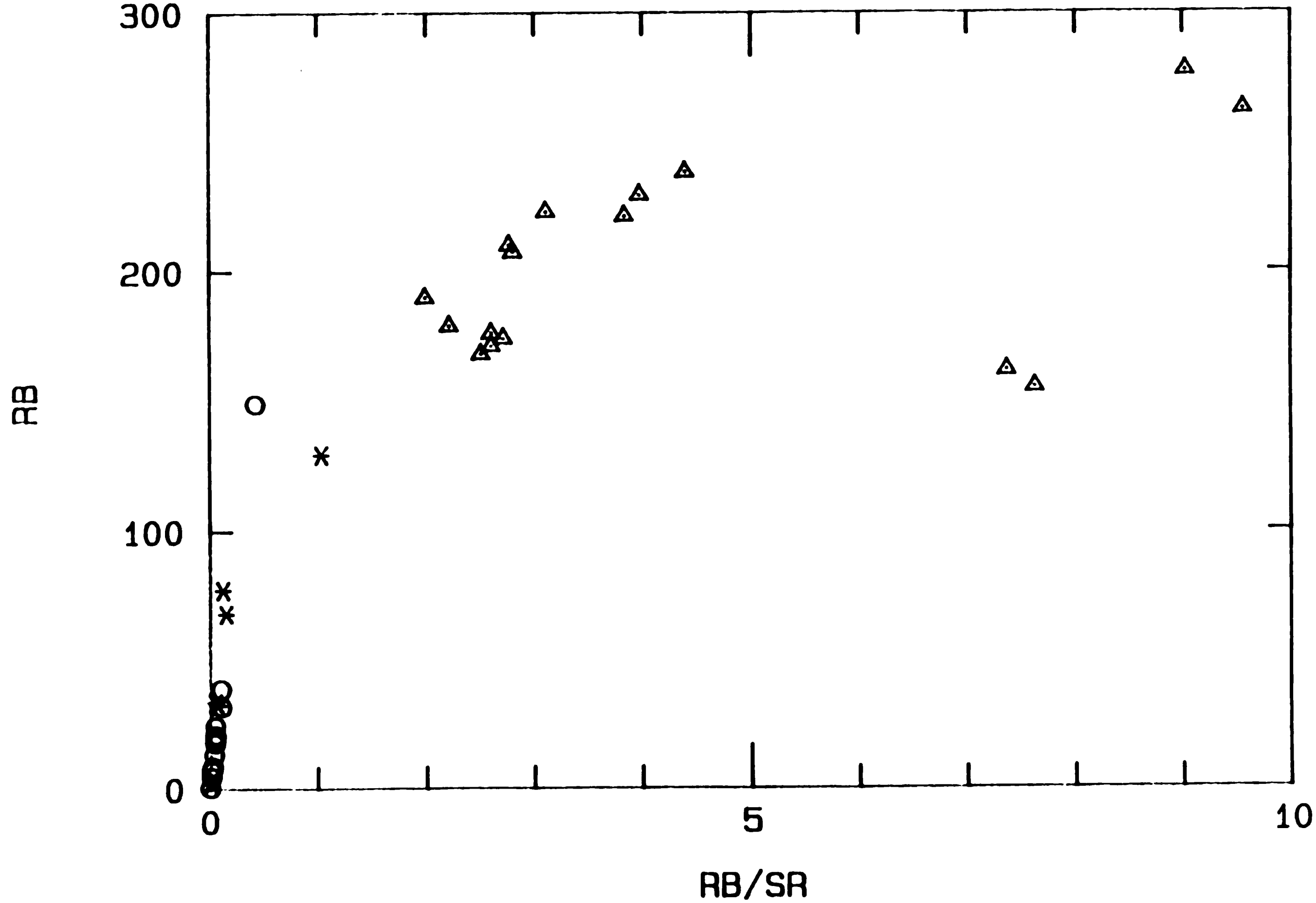

Figure 12
Potassic Metasomatism Assessment

degree of metasomatism. Correlation coefficients of the trace element data with K_2O and Fe_2O_3 is presented in Appendix G. It can be seen from this data that although the UF may have undergone some degree of metasomatism the only trace element distributions that may have been affected are Th and Sr.

It is evident that potassic metasomatism has taken place within the rhyolites of the UF. The basalts and andesites appear to be unaffected by it. The metasomatism does not however, affect the trace element distributions that are used herein to develop petrogenetic hypothesis.

DISCUSSION

Models for the development and evolution of the MCR have been presented by Miller (1986), Gordon and Hempton (1986), Green (1983) Wieblen and Morey (1980), Chase and Gilmer (1973), and Burke and Dewey (1973) among others. Green (1983) summarizes many of the previous models and presents his "preferred model".

In Greens model lavas were erupted into nine temporally and spatially separate plateaus that developed along the Lake Superior portion of the MCR. The plateaus were fed by numerous fissures, now occupied by dikes that parallel the MCR. The mechanism that begins this process is a heat source from a deep upwelling that caused the earliest primitive melts. As the convection lost its thermal impetus volcanism ceased abruptly.

Gordon and Hempton (1986) present evidence that the MCR formed as a result of convergence related to the synchronous Grenville Orogeny. The MCR formed due to the strike slip faults in the hinterland of the convergent strain. Extensional zones due to the sheer faults would form pull apart basins. Miller (1986) also appears to favor rift development as being syngenetic with the Grenville Orogeny.

Miller (1986) presents a petrochemical scheme for the development of the MCR volcanics. The volcanism occurs in three stages that appear to be present in Michigan 1) an early volcanism stage (PMG) 2) an anorthositic stage (PLL) and, 3) a troctolitic stage.

This study has shown through the use of petrographic analysis and major and trace element variations that the basalts and andesites of the UF are related through fractional crystallization of olivine, augite and plagioclase $\pm$ spinel. To account for the variation of incompatible trace elements within the basalts and andesites magma mixing with an evolved source must have occured. The same data has led to the conclusion that the rhyolites of the UF were formed due to partial melting. The partial melting occurred in more than one source and the melts were probably mixed with the more mafic magmas.

The rocks of the UF are interpreted as being the result of changing magmatic conditions within the MCR. The basalts and andesites were derived from the partial melting of a relatively evolved original source. These partial melts ponded in the crust and under went fractional crystallization. Changes in pressure, and/or temperature likely due to injection of new magma into the chamber resulted in the eruption of the basalts and andesites of the UF. The rhyolites were likely formed by wholesale or partial melting of the crust as it was heated by injection of the basaltic magma.

These conclusions are consistent with the hypothesis of Miller, 1986, presented above, and would correlate to a transition from his anorthositic stage to the troctolitic stage.

The nature and extent of the crustal melting within the troctolitic stage may provide valuable clues as to why the volcanic activity ceased so abruptly. Future studies of the UF should concentrate on the timing and nature of the crustal melting in order to gain an understanding of how this led to the failure of the rift.

CONCLUSIONS

-- The lavas of the Unnamed Formation are remnants of a Keweenawan age central volcanic complex.

-- The lavas of the Unnamed Formation were deposited during basin subsidence.

-- The rocks of the Unnamed Formation are calc alkaline to tholeitic and span the range of compositions from basalt to rhyolite.

-- Andesite and rhyolite are the dominant rock types at the center of the volcanic complex. The basaltic rocks are dominant on the flanks of the formation.

-- The felsic rocks make up 25% of the Unnamed Formation.

-- The felsic rocks contain SiO_2 up to 76.91%

-- The rocks of the Unnamed Formation have undergone low grade metamorphism.

-- The trace elements were relatively unaffected by the low grade metamorphism.

— The basalts and andesites were formed by fractional crystallization of olivine, plagioclase, and augite$\pm$ spinel along with magma mixing with a more evolved lava.

-- The rhyolites were formed by wholesale or partial melting of more than one evolved source. Which supports the hypothesis of Miller, 1986.

-- The rhyolitic lavas were likely the lavas that mixed with the more primitive basalt and andesite magmas.

LIST OF REFERENCES

Allegre, C.J. and Minster, J.F., 1978. Quantitative models of trace element behavior in magmatic processes. Earth and Planetary Science Letters, 38, 1-25.

Anderson, A.T. 1976. Magma Mixing: Petrological Process and Volcanologic Tool. Journal of Volcanology and Geothermal Research, 1: 3-33.

Books, K.G., 1972. Paleomagnetism of some Lake Superior Keweenawan lava flows in the Lake Superior area. United States Geologic Survey Professional Paper, 760, 42.

Brooks, E.R., and Garbutt P.L., 1969. Age and Genesis of Quartz-Porphery Near White Pine, Michigan. Economic Geology, v64:342-346.

Burke, K, and Dewey, J.F. 1973. Plume-generated Triple Junctions: Key Indicators in Applying PLate Tectonics to Old Rocks. J. Geology, v81:406-433.

Butler, J.C. and Woronow, A., 1986. Discrimination among tectonic settings using trace element abundances of basalts. Journal of Geophysical Research, 91, no. B10, 10,289-10,300.

Chase,C.G., and Gilmer, T.H., 1973. Precambrian PLate Tectonics: The Midcontinent Gravity high. Earth and Planetary Science Letters, v21:70-78.

Clague, D.A. and Frey, F.A., 1982. Petrology and trace element geochemistry of the Honolulu Volcanics, Oahu: Implications for the oceanic mantle below Hawaii. Journal of Petrology, 23, pt.3, 447-504.

Cox, K.G., Bell, J.D., and Pankhurst, R.J., 1979. The Interpretation of Igneous Rocks. George Allen & Unwin Limited, London. 450 p.

Gell, J.W., 1987. Geochemistry of the Lower Keweenawan Powder Mill Group, Upper Michigan. Masters Thesis, Michigan State University, 51p.

Gordon, M.D. and Hempton, M.R., 1986. Collision-induced rifting: The Grenville orogeny and the Keweenawan rift of North America. Tectonophysics, 127, 1-25.

Green, J.C., 1983. Geologic and geochemical evidence for the nature and development of the Middle Proterozoic (Keweenawan) Midcontinent rift of North America. In: Processes of continental rifting. P. Morgan and B.H. Baker (editors). Tectonophysics, 94, 413-437.

Green, J.C., 1982. Geology of Keweenawan extrusive rocks. In: Geology and tectonics of the Lake Superior Basin. Wold, R.J. and Hinze, W.J. (editors). Geologic Society of America Memoir, 156,280 p.

Green, T.H. and Pearson, N.J., 1987. An experimental study of Nb and Ta partitioning between Ti-rich minerals and silicate liquids at high pressures and temperatures. Geochimica et Cosmocimica Acta, 51, 55-62.

Hanson, G.N. and Langmuir, C.N., 1978. Modeling of Major Elements in Mantle-Melt systems using Trace Element Approaches. Geochim Cosmochim Acta 50: 1551-1557.

Harker, A., 1909. <u>The Natural History of Igneous Rocks</u>. New York: McMillan.

Hubbard, H.A., 1975a. Keweenawan Geology of the North Ironwood, Ironwood and Little Girls Point Quadrangles, Gogebic County, Michigan. U.S. Geologic Survey, Open File Report, 75-152.

Hubbard, H.A., 1975b. Geology of the Porcupine Mountians in the Carp River and White Pine Quadrangles, Michigan. U.S. Geologic Survey, Journal of Research, v3, n5, 519-528.

Huppert, H.E., and Sparks, R.S.J., 1984. Double-diffusion convection due to crystallization in magmas. Annual Review of Earth and Planetary Sciences, 12, 11-37.

Irving, R.D., 1883. The copper-bearing rocks of Lake Superior. United States Geologic Survey Monograph, 5, 464 p.

Irving, T.N. and Barager, W.R.A., 1971. A guide to the chemical classification of the common volcanic rocks. Canadian Journal of Earth Sciences, 8, 523-548.

Johnson, R.F., and White, W.S., 1969. Preliminary Report on the Bedrock Geology and Copper Deposits of the Matchwood Quadrangle, Ontonagon County, Michigan. U.S. Geological Survey, Open File Report.

King, E.R., 1975. A typical cross section based on magnetic data of Lower and Middle Keweenawan volcanic rocks, Ironwood area, Michigan. United State Geologic Survey Journal Research, 3, 543-546.

Kopledowski, P.J., 1983. The Oak Bluff Volcanics, A Middle Keweenawan Central Volcano; Porcupine Mountians Region, Michigan. Masters Thesis, 88 p.

Langmuir, C.H., Vocke, R.D., Hanson, G.N., and Hart, S.R., 1978. A general mixing equation with applications to Icelandic basalts. Earth and Planetary Science Letters, 37, 380-392.

Masey, N.W.D., 1983. Magma Genesis in a Late Proterozoic Proto-Oceanic Rift: REE and Other Trace Element Data from the Keweenawan Mamainse Point Formation, Ontario, Canada. Precambrian Research, v21:81-100.

Miller, J.D., 1986. The geology and petrology of anorthositic rocks in the Duluth Complex, Snowbank Lake quadrangle, Northeastern Minnesota. Doctoral dissertation, University of Minnesota, 436 p.

Minster, J.F. and Allegre, C.J., 1978. Systematic use of trace elements in igneous processes. Part III. Inverse problem of batch partial melting in volcanic suites. Contributions in Mineralogy and Petrology, 68, 37-52.

Minster, J.F., Minster, J.B., Treuil, M., and Allegre, C.F., 1977. Systematic use of trace elements in igneous processes. Part II. Inverse problem of the fractional crystallization processes in volcanic suites. Contributions to Mineralogy and Petrology, 61, 40-77.

O'Hara, M.J. and Mathews, R.E., 1981. Geochemical evolution in an advancing, periodically replenished, periodically tapped, continuously fractionated magma chamber. Journal of the Geologic Society of London, 138, 237-277.

Paces, J.B., 1988. Magmatic Processes, Evolution and Mantle Source Characteristics Contributing to the Petrogenesis of Midcontinent Rift Basalts: Portage Lake Volcanics, Keweenaw Peninsula, Michigan. Doctoral Dissertation, Michigan Technological University, 413p.

Palmer, H.C. and Halls, H.C., 1985. The paleomagnetism of the Powder Mill Group: Its relevance to correlation with other Keweenawan sequences and to tectonic development of the south range. Abstracts for the 31st annual Institute on Lake Superior Geology, 73.

Pearce, T.H., 1969. A Contribution to the Theory of Variation Diagrams. Contributions to Mineralogy and Petrology, v19:142-157.

Stanley, C.R., and Russell, J.K., 1988. Pearce.plot: A Turbo Pascal Program for the Analysis of Rock Compositions With Pearce Element Ratio Diagrams. submitted to Computers and Geosciences.

Thompson, R.N., Dickin, A.P., Gibson, I.L., and Morrison, M.A., 1982. Elemental fingerprints of isotopic contamination of Hebridean Ipaleocene mantle-derived magmas by Archean sial. Contributions to Mineralogy and Petrology, 79, 159-168.

Treuil, M., 1973. Criteres petrologiques et structuraux de la genese et de la differenciation des magmas basaltiques. Exemple de l'Afar. These Orleans.

Treuil, M. and Joron, J.L., 1975. Utilisation des elements hygromagmatophiles pour la simplification de la modelisation quantitative des processus magmatiques. Examples de l'Afar et de la dorsale methioatlantique. Society of Italian Mineralogy and Petrology, 31, 125-174.

Wasuwanich, P., 1979. Models of basalt petrogenesis: A study of Lower Keweenawan diabase dikes and Middle Keweenawan Portage Lake Lavas, Michigan. Master's Thesis. 71 p.

Wieblen, P.W., and Morey, G.B., 1980. A Summary of the Stratigraphy, Petrology, and Structure of the Duluth Complex. American Journal of Science, v280a:88-133.

Wilband, J.T., 1984. Age and source variation of volcanics associated with Keweenawan Rifting. Transactions of the American Geophysical Union, 65, 1122.

Wilband, J.T. and Wasuwanich, P., 1980. Models of basalt petrogenesis: Lower Keweenawan diabase dikes and Middle Keweenawan Portage Lake Lavas, Upper Michigan. Contributions to Mineralogy and Petrology, 75, 395-406.

Whitlow, J.W., 1974. Geologic map of the Greenland and Rockland Quadrangles, Ontonagon County, Michigan. U.S. Geologic Survey, Misc. Field Studies, Map MF 596.

Wold, R.J., and Hinze, W.J., 1982. Geology and Tectonics of the Lake Superior Basin. Geological Society of America, Memoir 156.

Yoder, H.S., 1976. Generation of basaltic magma. National Academy of Sciences, Washington, D.C., 265 p.

Appendix A

Sample Locations

Appendix A

SAMPLE LOCATIONS

SAMPLE	TOWNSHIP	RANGE	SECTION	1/4	1/4	1/4
TQ-1	48N	45W	20	SW	SE	SW
TQ-2	48N	45W	20	SW	SE	SW
TQ-3	48N	45W	20	NW	SE	SW
TQ-4	48N	45W	20	NW	SE	SW
TQ-5	48N	45W	29	SE	SW	NE
TQ-6	49N	44W	20	NE	NE	NW
BQ-1	49N	42W	10	SW	SW	SW
BQ-2	49N	42W	15	NW	NW	NW
BQ-3	49N	42W	15	SW	NW	NW
BQ-4	49N	42W	15	SW	NW	NW
BQ-5	49N	42W	15	NW	SW	NW
BQ-6	49N	42W	15	NW	SW	NW
BQ-7	49N	42W	15	SW	SW	NW
BQ-8	49N	42W	15	SW	SW	NW
MNW-1	50N	41W	21	NE	SE	SW
MNW-2	50N	41W	21	NE	SE	SW
MNW-3	50N	41W	21	NE	SE	SW
MNW-4	50N	41W	21	NE	SE	SW
MNW-5	50N	41W	21	NE	SE	SW
MNW-6	50N	41W	21	NE	SE	SW
MNW-7	48N	41W	12	SW	SW	NW
MNW-8	48N	41W	12	SW	SW	NW
MNW-9	48N	41W	11	SE	SE	NE
MNW-10	50N	41W	24	SE	SW	NW
MNW-11	50N	41W	24	SE	SW	NW
MNW-12	50N	41W	24	SW	SW	NW
MNW-12.5	50N	41W	24	NE	SW	NW
MNW-13	50N	41W	24	NE	SW	NW
LC-1	50N	45W	14	NE	NE	NE
LC-2	50N	45W	14	SW	SW	NW
LC-3	50N	45W	13	SW	SW	NE
LC-4	50N	45W	13	NE	SE	SE
NIQ-1	48N	46W	32	NW	NW	SW
NIQ-2	48N	46W	32	NW	NW	SW
NIQ-3	48N	46W	32	NW	NW	SW
NIQ-4	48N	46W	32	NW	NW	SW
NIQ-5	48N	46W	32	NW	NW	SW
NIQ-6	48N	46W	32	NW	NW	SW
NIQ-7	48N	46W	32	SW	NE	NE
NIQ-8	48N	46W	28	SW	SW	SW
NIQ-9	48N	46W	28	SW	SW	SW
NIQ-10	48N	46W	29	SE	SE	SE
NIQ-11	48N	46W	29	SE	SE	SE
NI-1	48N	46W	28	SW	SW	SW
NI-2	48N	46W	29	SE	SE	SE
JWCF-9	48N	46W	32	SE	SE	NW

Appendix A
(Continued)

SAMPLE LOCATIONS

SAMPLE	TOWNSHIP	RANGE	SECTION	1/4	1/4	1/4
JWCF-10	48N	46W	32	NE	NE	SW
JWUN-13	48N	44W	19	SW	SW	NW
JWUN-14	48N	44W	19	SW	SW	NW
JWUN-16	49N	42W	4	NE	NW	SW
CC-1	49N	43W	18	SE	SE	NE
CC-2	49N	43W	18	SE	SE	NE
CC-3	49N	43W	18	SE	SE	NE
CC-4	49N	43W	18	SE	SE	NE
CC-5	49N	43W	18	SW	SE	NE
CC-6	49N	43W	18	SW	SE	NE
CC-7	49N	43W	18	SW	SE	NE
JQ-1	49N	42W	15	NW	NW	NW
JQ-2	49N	42W	15	NW	NW	NW
JQ-3	49N	-42W	15	NW	NW	NW
JWUF-12	49N	44W	16	NW	SW	NW

Appendix B

Analytical Methods

Appendix B

Analytical Methods

The bulk rock chemistry was determined using X-ray fluorescence and Instrumental Neutron Activation Analysis (INAA). Samples were slabbed, trimmed of any weathered rind and secondary mineralization, and ground into a homogenous powder (200 mesh). Powdered samples were dried in an evacuated oven at 50°C for 24 hours to remove nonstructural water.

For X-ray fluorescence analysis two types of sample preparation were used. Glass wafers were made using 1.0000 gram of dried sample, 9.0000 grams of lithium tetraborate, and 0.160 grams of ammonium nitrate. This mixture was liquified by firing for thirty minutes at about 1100°C. The mixture was poured into a mold and slowly cooled. The glass wafers were used to analyze for Si, Al, Fe, Mg, Ca, Na, K, Ti, P and Mn.

Analysis for trace elements Cr, Ni, Cu, Zn, Rb, Sr, Y, Zr, Nb and La by X-ray fluorescence were done using pressed powdered pellets.

INAA was conducted using 1.00000 gram powdered samples in sealed polyvinyl vials. Samples were irradiated for about 18 hours over a three day period. Elements analyzed were La, Ce, Sm, Eu, Tb, Yb, Lu, Hf, Th and Cr.

Appendix C

Average Modal Percentages of Minerals in Thin Section

Appendix C

AVERAGE MODAL PERCENTAGES OF MINERALS IN THIN SECTION

	OLIVINE	AUGITE	OPAQUES	PLAGIOCLASE	ALBITE	QUARTZ
BASALT	10	20	20	50		
ANDESITE	5	10		85		
RHYOLITE				60	10	30

Appendix D

Chemical Analysis

Appendix D

Chemical Analysis

	NIQ-1	CC-4	NI-2	NIQ-3	NIQ-2	CC-5	TQ-4	CC-7	TQ-2	TQ-3	JWUN-15	NIQ-7	JWUN-16
SiO2	44.25	47.38	47.49	47.61	47.67	48.03	48.14	48.14	48.22	48.63	48.98	49.33	49.34
TiO2	1.81	2.05	2.02	1.49	1.40	2.00	0.82	1.97	0.92	0.96	1.92	1.68	1.48
Al2O3	16.41	15.59	16.53	16.50	16.40	15.36	17.05	15.59	16.62	16.14	15.32	14.00	15.76
Fe2O3	3.94	10.69	7.82	6.10	5.87	11.10	1.67	5.04	0.71	1.59	7.16	5.77	9.01
FeO	10.36	2.42	4.19	5.67	5.75	2.48	9.51	6.69	9.89	9.76	4.67	7.13	2.54
MnO	0.24	0.16	0.17	0.16	0.17	0.16	0.16	0.20	0.16	0.17	0.14	0.22	0.13
MgO	7.28	4.80	6.05	6.90	7.46	5.13	8.27	7.07	8.22	7.97	4.94	5.35	6.31
CaO	8.92	9.48	7.65	9.56	9.12	8.41	10.55	7.99	11.10	10.93	8.37	8.39	9.64
Na2O	2.34	2.49	3.07	2.22	2.22	2.56	2.11	3.27	2.01	2.03	2.37	3.78	1.99
K2O	0.80	1.08	1.55	0.50	2.30	1.11	0.37	0.49	0.38	0.40	1.01	1.09	0.16
P2O5	0.26	0.57	0.48	0.27	0.25	0.56	0.14	0.48	0.16	0.16	0.45	0.23	0.22
H2O+	2.61	2.06	2.26	2.76	0.00	2.08	0.32	2.39	0.90	0.41	4.08	1.67	2.82
H2O-	0.00	0.00	0.00	0.00	0.00	0.00	0.00	0.00	0.00	0.00	0.00	0.00	0.00
	-----	-----	-----	-----	-----	-----	-----	-----	-----	-----	-----	-----	-----
TOTAL	99.22	98.77	99.28	99.74	98.61	98.98	99.11	99.32	99.29	99.15	99.41	98.64	99.40
Ni	138.1	114.6	89.4	180.7	188.0	113.0	105.4	103.2	121.7	101.2	81.7	47.2	150.1
Cu	97.5	27.6	75.0	106.4	47.6	30.2	36.2	83.3	34.4	35.5	41.4	57.4	502.6
Zn	125.8	128.1	140.6	105.8	105.0	141.8	77.6	114.8	80.5	80.8	120.4	112.0	77.5
Sr	354.1	395.0	494.9	323.4	323.9	426.1	360.9	490.3	331.3	339.4	372.9	298.7	326.1
Rb	13.5	19.7	24.6	8.1	8.9	21.2	7.4	7.7	7.9	8.7	18.0	32.1	0.7
Y	29.9	37.1	40.2	24.9	23.5	37.1	17.5	31.3	18.1	19.9	36.8	35.6	22.5
Zr	166.7	283.6	313.7	140.8	132.0	285.1	90.3	221.8	93.9	101.0	293.3	179.6	132.5
Nb	8.0	16.0	12.6	7.4	7.0	15.0	4.3	12.8	4.3	4.9	12.9	8.4	5.4
Ba	508.2	864.6	1113.4	427.1	460.8	1144.7	288.1	451.0	316.6	339.7	866.9	519.9	298.9
La	18.7	43.5	35.9	22.3	12.1	35.9	31.1	32.4	29.7	26.5	46.5	15.9	25.7
Sm	5.30	8.73	9.61	0.00	4.57	8.87	0.00	6.45	0.00	0.00	8.72	6.09	4.74
La	22.88	64.62	61.39	0.00	19.91	58.19	0.00	34.93	0.00	0.00	63.68	24.02	24.01
Ce	50.90	116.07	120.61	0.00	48.49	106.74	0.00	75.43	0.00	0.00	117.68	63.56	44.07
Yb	2.43	3.14	4.43	0.00	2.33	3.53	0.00	3.87	0.00	0.00	4.26	3.30	2.16
Lu	0.39	0.43	0.70	0.00	0.39	0.47	0.00	0.42	0.00	0.00	0.58	0.51	0.38
Cr	139.40	163.77	95.29	0.00	189.71	148.11	0.00	176.21	0.00	0.00	115.09	113.71	251.21
Hf	3.78	6.02	6.98	0.00	3.26	6.54	0.00	6.17	0.00	0.00	5.85	4.67	2.98
Th	3.00	4.23	6.66	0.00	2.81	4.99	0.00	2.77	0.00	0.00	6.48	2.59	1.64
Eu	1.81	2.76	2.72	0.00	1.33	2.47	0.00	2.05	0.00	0.00	2.25	1.88	1.55
Tb	1.05	1.42	0.97	0.00	0.89	0.83	0.00	1.08	0.00	0.00	1.03	0.64	1.03
La/Yb	9.42	20.58	13.86	ERR	8.55	16.48	ERR	9.03	ERR	ERR	14.95	7.28	11.12

Appendix D
(Continued)

Chemical Analysis

	JMCF-10	NIB-10	JMCF-9	MMW-11	LC-1	CC-1	MMW-12	LC-2	CC-6	CC-2	CC-3	NIB-5	NIB-4
SiO2	49.96	50.14	50.27	50.98	51.30	51.59	52.77	53.41	53.61	54.39	55.27	57.41	60.14
TiO2	1.44	1.43	1.72	2.92	1.67	1.63	2.73	1.51	0.91	1.53	1.52	2.26	2.41
Al2O3	16.24	15.10	14.04	12.75	15.52	15.14	13.03	15.13	15.75	14.84	14.91	11.05	8.82
Fe2O3	4.74	5.08	11.16	9.78	5.99	7.38	8.59	7.22	3.30	5.92	4.55	7.28	8.12
FeO	6.09	6.04	1.94	4.19	5.05	4.36	4.17	3.83	6.66	4.43	4.61	2.34	1.79
MnO	0.15	0.16	0.17	0.17	0.14	0.15	0.19	0.14	0.17	0.16	0.18	0.12	0.09
MgO	6.54	6.57	5.85	3.20	5.90	4.66	3.79	5.36	6.46	4.18	4.99	2.73	1.94
CaO	9.77	7.54	5.74	5.77	7.17	8.83	4.21	5.62	4.78	5.46	5.75	10.34	12.01
Na2O	2.06	2.73	4.01	2.75	2.46	2.56	3.06	3.00	3.77	2.86	2.99	1.51	0.08
K2O	0.38	1.23	2.35	2.92	1.60	1.17	2.78	2.02	1.50	3.09	2.06	0.47	0.09
P2O5	0.26	0.28	0.28	1.35	0.37	0.38	1.13	0.34	0.08	0.41	0.40	0.20	0.21
H2O+	1.88	3.05	1.61	1.57	1.69	0.87	2.14	1.89	2.45	2.05	1.90	4.24	4.03
H2O-	0.00	0.00	0.00	0.00	0.00	0.00	0.00	0.00	0.00	0.00	0.00	0.00	0.00
TOTAL	99.51	99.35	99.14	98.35	98.86	98.72	98.59	99.47	99.44	99.32	99.13	99.95	99.73
Ni	175.0	118.9	88.7	0.0	85.8	77.9	0.0	85.8	62.3	55.9	56.1	48.7	51.4
Cu	79.7	45.1	9.0	0.0	26.5	43.1	0.0	28.7	73.6	18.2	49.4	203.2	51.7
Zn	100.2	120.8	108.7	0.0	113.8	100.3	0.0	113.0	88.6	119.9	119.1	123.1	125.1
Sr	318.3	425.1	331.5	0.0	374.4	394.5	0.0	449.7	665.5	630.7	446.0	387.2	496.3
Rb	4.9	20.9	149.0	0.0	38.9	20.9	0.0	67.9	33.8	77.1	32.7	3.0	2.3
Y	24.0	30.7	56.4	0.0	42.4	6.5	0.0	43.6	26.7	51.7	44.1	31.3	30.7
Zr	135.7	182.0	190.6	0.0	302.4	289.8	0.0	281.4	132.3	404.2	398.7	280.2	274.3
Nb	7.1	8.3	11.2	0.0	12.1	16.8	0.0	12.0	5.0	15.5	17.3	20.3	19.7
Ba	328.8	710.1	922.1	0.0	833.3	72.9	0.0	939.7	538.6	1156.7	1076.3	172.9	125.5
La	19.1	16.1	13.3	0.0	55.2	0.0	0.0	35.1	25.2	61.8	69.7	0.1	5.2
Sc	4.74	6.08	5.77	15.18	0.00	8.62	14.41	7.96	3.66	10.96	10.42	7.36	7.41
La	25.22	30.97	26.09	76.63	0.00	54.01	79.46	54.79	17.67	78.98	77.58	33.34	28.80
Ce	46.22	62.63	57.81	150.95	0.00	100.89	149.04	95.71	39.33	140.95	145.77	67.74	66.39
Yb	2.00	2.68	3.04	6.06	0.00	4.38	4.62	2.40	2.24	4.54	3.30	2.75	4.10
Lu	0.34	0.34	0.48	0.68	0.00	0.61	0.70	0.51	0.31	0.48	0.49	0.33	0.56
Cr	189.93	135.34	150.83	22.26	0.00	96.91	5.93	88.69	28.65	73.43	59.60	90.93	100.90
Hf	3.09	4.46	4.30	10.19	0.00	5.36	10.44	5.11	2.64	9.12	9.11	6.88	6.70
Th	2.08	5.46	4.69	8.80	0.00	5.71	8.64	4.65	7.15	12.94	12.39	5.43	4.76
Eu	1.51	1.76	1.46	4.17	0.00	2.08	4.41	2.11	1.12	2.20	2.39	1.90	2.01
Tb	1.01	1.27	1.11	1.59	0.00	1.23	2.23	0.69	1.07	0.97	1.30	1.12	0.90
La/Yb	12.61	11.56	8.58	12.65	ERR	12.33	17.20	22.83	7.89	17.40	23.51	12.12	7.02

Appendix D
(Continued)

Chemical Analysis

	TQ-5	NI-1	BQ-4	BQ-8	MNW-2	BQ-6	BQ-7	JQ-3	MNW-1	MNW-5	MNW-6	JQ-1	MNW-4
SiO_2	65.54	70.34	71.34	71.42	71.62	71.92	72.09	72.40	72.55	72.74	73.42	73.61	73.70
TiO_2	0.63	0.30	0.27	0.28	0.39	0.26	0.26	0.37	0.29	0.30	0.33	0.32	0.34
Al_2O_3	13.37	13.54	13.14	13.24	12.19	13.29	13.29	11.93	11.88	11.97	11.86	11.52	11.64
Fe_2O_3	7.16	3.20	2.54	1.99	4.38	2.05	1.53	3.74	3.67	3.32	3.50	3.69	3.15
FeO	0.11	0.26	0.94	0.89	0.26	0.74	0.75	0.26	0.20	0.21	0.12	0.47	0.32
MnO	0.14	0.03	0.04	0.04	0.08	0.04	0.04	0.05	0.06	0.05	0.06	0.07	0.06
MgO	0.41	0.24	0.54	0.43	0.80	0.37	0.38	0.52	0.36	0.42	0.41	0.53	0.33
CaO	1.95	0.18	0.52	0.88	0.21	0.81	0.90	0.43	0.14	0.14	0.22	0.19	0.21
Na_2O	3.76	2.10	2.76	2.98	1.09	3.18	3.11	1.60	1.12	0.83	1.60	1.94	1.74
K_2O	4.38	8.94	5.93	6.00	7.56	5.88	5.91	7.10	8.20	8.91	7.22	6.27	6.99
P_2O_5	0.11	0.01	0.05	0.05	0.04	0.04	0.05	0.05	0.01	0.01	0.05	0.03	0.04
H_2O+	0.73	0.47	1.04	1.04	1.10	0.96	0.99	0.97	0.75	0.59	1.05	0.77	0.61
H_2O-	0.00	0.00	0.00	0.00	0.00	0.00	0.00	0.00	0.00	0.00	0.00	0.00	0.00
TOTAL	98.29	99.61	99.01	99.24	99.72	99.54	99.30	99.42	99.23	99.49	99.86	99.41	99.13
Ni	6.6	18.0	17.3	6.3	14.3	6.5	7.2	0.0	15.8	0.0	0.0	14.3	18.4
Cu	17.1	43.8	8.2	6.2	33.6	7.7	7.7	0.0	20.5	0.0	0.0	21.8	22.5
Zn	97.0	162.1	93.8	68.3	281.6	62.0	67.8	0.0	145.7	0.0	0.0	181.9	123.7
Sr	125.2	27.4	67.2	64.2	76.0	67.8	65.9	0.0	74.1	0.0	0.0	95.6	81.0
Rb	129.4	262.1	168.1	174.1	210.3	176.1	171.2	0.0	207.6	0.0	0.0	189.9	178.9
Y	75.3	171.7	78.7	70.7	118.5	63.4	68.1	0.0	138.5	0.0	0.0	114.6	128.1
Zr	974.1	1095.9	321.5	337.7	1133.2	311.5	315.8	0.0	1279.2	0.0	0.0	1071.9	1009.3
Nb	27.2	33.6	29.4	29.1	34.3	26.9	28.5	0.0	36.7	0.0	0.0	33.8	33.3
Ba	3096.5	940.4	1320.9	956.3	362.1	924.6	899.4	0.0	404.4	0.0	0.0	291.8	353.8
La	0.0	0.0	208.4	0.0	0.0	0.0	0.0	0.0	0.0	0.0	0.0	0.0	0.0
Sm	16.48	25.49	15.79	15.13	22.58	0.00	0.00	22.54	30.08	27.30	17.81	21.25	22.70
La	117.96	270.36	163.37	144.59	218.80	0.00	0.00	210.03	334.39	243.52	121.83	212.18	145.15
Ce	202.63	496.53	251.24	224.23	317.20	0.00	0.00	489.59	552.98	515.02	360.89	307.15	544.95
Yb	7.60	7.63	7.59	5.36	8.05	0.00	0.00	6.98	8.40	7.24	6.67	7.08	6.95
Lu	1.20	1.22	0.92	0.71	1.31	0.00	0.00	1.06	1.42	1.16	1.06	1.09	1.16
Cr	9.30	29.07	10.12	1.40	2.13	0.00	0.00	8.85	5.23	13.20	6.26	47.77	37.36
Hf	18.93	24.12	9.42	8.96	21.73	0.00	0.00	21.89	24.55	26.26	21.23	23.16	21.98
Th	21.05	45.77	29.58	28.83	36.41	0.00	0.00	33.63	36.73	37.20	34.56	36.67	33.67
Eu	6.87	3.01	1.62	1.84	1.63	0.00	0.00	1.77	1.52	1.33	1.62	1.49	1.70
Tb	1.22	3.28	1.22	1.08	1.74	0.00	0.00	2.84	2.11	2.90	2.66	2.66	2.95
La/Yb	15.52	35.43	21.52	26.98	27.18	ERR	ERR	30.09	39.81	33.64	18.27	29.97	20.88

Appendix D
(Continued)

Chemical Analysis

	JWUN-14	BQ-9	JQ-3	BQ-2	BQ-1	JWUF-12	LC-3	LC-4	NIQ-8
SiO_2	74.23	74.71	74.75	74.77	75.07	75.73	76.36	76.44	76.91
TiO_2	0.17	0.19	0.23	0.18	0.19	0.16	0.15	0.14	0.14
Al_2O_3	11.96	13.02	11.32	12.91	12.58	11.24	11.17	10.62	10.59
Fe_2O_3	2.00	1.30	2.59	0.94	0.89	2.46	2.18	2.21	2.11
FeO	0.21	0.34	0.34	0.34	0.36	0.21	0.09	0.13	0.15
MnO	0.04	0.02	0.05	0.02	0.01	0.02	0.03	0.04	0.02
MgO	0.08	0.27	0.31	0.18	0.26	0.09	0.22	0.08	0.05
CaO	0.31	0.81	0.13	0.75	0.74	0.20	0.13	0.31	0.13
Na_2O	3.19	3.19	1.01	2.09	2.16	1.67	0.57	0.18	0.30
K_2O	5.67	5.39	7.97	6.61	6.35	7.13	8.58	9.19	9.55
P_2O_5	0.01	0.03	0.02	0.03	0.03	0.00	0.00	0.00	0.00
H_2O+	0.27	1.80	0.60	1.29	1.26	0.33	0.67	0.53	0.26
H_2O-	0.00	0.00	0.00	0.00	0.00	0.00	0.00	0.00	0.00
TOTAL	98.14	101.07	99.32	100.11	99.90	99.24	100.15	99.87	100.21
Ni	13.5	5.9	15.3	9.2	8.0	10.9	12.3	12.1	10.8
Cu	6.9	8.1	27.2	7.6	10.1	23.6	49.2	28.7	9.7
Zn	63.5	45.4	135.8	26.1	24.1	135.7	132.9	92.5	41.7
Sr	21.9	77.1	71.9	57.8	57.8	30.7	54.3	20.3	13.0
Rb	161.4	567.6	223.2	229.7	221.5	277.2	238.4	154.9	227.6
Y	94.5	197.9	134.1	79.5	78.6	116.4	95.0	95.9	112.7
Zr	606.1	68.5	882.1	217.6	214.3	544.6	536.3	537.2	504.2
Nb	31.4	204.0	35.7	24.0	23.6	31.4	32.8	35.5	30.4
Ba	1369.6	23.2	367.0	649.6	640.3	72.8	142.5	136.0	907.6
La	0.0	1197.6	0.0	0.0	0.0	0.0	0.0	0.0	0.0
Sm	0.00	0.00	18.86	0.00	12.37	13.98	7.65	16.37	11.83
La	0.00	0.00	141.60	0.00	111.27	94.35	31.74	94.16	75.11
Ce	0.00	0.00	292.75	0.00	192.52	168.08	201.07	160.41	161.53
Yb	0.00	0.00	6.69	0.00	4.88	5.26	7.22	7.59	5.77
Lu	0.00	0.00	1.00	0.00	0.59	0.76	1.09	1.08	0.83
Cr	0.00	0.00	9.28	0.00	0.04	5.10	9.34	1.48	3.81
Hf	0.00	0.00	20.33	0.00	7.17	14.72	14.51	14.06	15.21
Th	0.00	0.00	37.45	0.00	29.50	38.32	40.67	36.13	29.62
Eu	0.00	0.00	0.97	0.00	1.23	0.34	0.16	0.45	0.92
Tb	0.00	0.00	2.67	0.00	0.80	1.98	1.19	1.24	2.04
La/Yb	ERR	ERR	21.17	ERR	22.80	17.94	4.40	12.41	13.02

Appendix E

CIPW Normative Analysis

Appendix E

CIPW NORMATIVE ANALYSIS

Sample	NIQ-1	CC-4	NI-2	NIQ-3	NIQ-2	CC-5	TQ-4	CC-7	TQ-2	TQ-3	JWUN-1	NIQ-7	JWUN-1	JWCF-1	NIQ-10
Group #	1.00	1.00	1.00	1.00	1.00	1.00	1.00	1.00	1.00	1.00	1.00	1.00	1.00	1.00	1.00
Qual	1	1	1	5	1	1	5	1	5	5	1	1	1	1	1
Key	0	0	0	0	0	0	0	0	0	0	0	0	0	0	0
Ref	1	1	1	1	1	1	1	1	1	1	1	1	1	1	1
SiO_2	45.99	49.54	49.35	49.40	48.63	50.14	48.81	49.92	49.04	49.33	51.77	51.18	51.57	51.42	52.34
TiO_2	1.88	2.14	2.10	1.55	1.43	2.09	0.83	2.04	0.94	0.97	2.03	1.74	1.55	1.48	1.49
Al_2O_3	17.06	16.30	17.18	17.12	16.73	16.04	17.29	16.17	16.90	16.37	16.19	14.52	16.47	16.72	15.76
FeO	14.46	12.60	11.68	11.59	11.26	13.03	11.17	11.65	10.71	11.35	11.75	12.79	11.14	10.66	11.08
MnO	0.25	0.17	0.18	0.17	0.17	0.17	0.16	0.21	0.16	0.17	0.15	0.23	0.14	0.15	0.17
MgO	7.57	5.02	6.29	7.16	7.61	5.36	8.39	7.33	8.36	8.08	5.22	5.55	6.59	6.73	6.86
CaO	9.27	9.91	7.95	9.92	9.30	8.78	10.70	8.29	11.29	11.09	8.85	8.70	10.08	10.06	7.87
Na_2O	2.43	2.60	3.19	2.30	2.26	2.67	2.14	3.39	2.04	2.06	2.50	3.92	2.08	2.12	2.85
K_2O	0.83	1.13	1.61	0.52	2.35	1.16	0.38	0.51	0.39	0.41	1.07	1.13	0.17	0.39	1.28
P_2O_5	0.27	0.60	0.50	0.28	0.26	0.58	0.14	0.50	0.16	0.16	0.48	0.24	0.23	0.27	0.29
Total	100.00	100.00	100.00	100.00	100.00	100.00	100.00	100.00	100.00	100.00	100.00	100.00	100.00	100.00	100.00
AN	61.71	57.21	50.73	64.13	59.84	55.62	66.82	48.84	67.43	66.27	58.43	36.03	66.61	66.07	52.29
Q	0.00	1.51	0.00	0.41	0.00	2.05	0.00	0.00	0.00	0.00	5.44	0.00	5.93	4.96	1.98
or	4.73	6.38	9.16	2.95	13.59	6.56	2.19	2.90	2.25	2.36	5.97	6.44	0.95	2.25	7.27
ab	19.80	21.07	25.98	18.79	18.79	21.66	17.85	27.67	17.01	17.18	20.05	31.99	16.84	17.43	23.10
an	31.91	28.17	26.75	33.58	27.99	27.14	35.96	26.42	35.21	33.75	28.18	18.02	33.60	33.95	25.32
di	8.75	12.46	6.56	9.85	12.71	9.00	12.66	8.18	15.45	15.94	8.52	18.25	10.43	10.44	8.36
hy	5.81	16.04	11.01	23.30	2.64	19.56	16.06	18.98	14.66	18.60	17.15	5.37	20.59	20.84	22.45
ol	16.71	0.00	7.08	0.00	15.15	0.00	9.76	2.75	10.67	6.41	0.00	8.32	0.00	0.00	0.00
mt	4.80	5.15	5.10	4.34	4.20	5.07	2.42	5.03	1.03	2.31	4.96	4.61	4.32	4.26	4.25
il	3.44	3.89	3.84	2.83	2.66	3.80	1.56	3.74	1.75	1.82	3.65	3.19	2.81	2.73	2.72
ap	0.60	1.32	1.11	0.63	0.58	1.30	0.32	1.11	0.37	0.37	1.04	0.53	0.51	0.60	0.65
FeO*	14.46	12.60	11.68	11.59	11.26	13.03	11.17	11.65	10.71	11.35	11.75	12.79	11.14	10.66	11.08
F/F+M	0.660	0.718	0.653	0.621	0.600	0.711	0.575	0.618	0.565	0.588	0.695	0.701	0.631	0.616	0.621
den	2.76	2.70	2.68	2.70	2.69	2.70	2.71	2.69	2.71	2.71	2.67	2.68	2.68	2.68	2.66

Appendix E
(Continued)

CIPW Normative Analysis

Sample	JWCF-9	MNW-11	LC-1	CC-1	MNW-12	LC-2	CC-6	CC-2	CC-3	NIQ-5	NIQ-4	TQ-5	NI-1	BQ-4	BQ-8
Group #	1.00	1.00	1.00	1.00	2.00	2.00	2.00	2.00	2.00	2.00	2.00	2.00	3.00	3.00	3.00
Qual	1	1	5	1	1	1	1	1	1	1	1	1	1	1	1
Key	0	0	0	0	1	1	1	1	1	1	1	1	5	5	5
Ref	1	1	1	1	1	1	1	1	1	1	1	1	1	1	1
SiO_2	52.14	53.21	53.12	53.12	55.20	55.14	55.46	56.26	57.11	60.44	63.38	67.68	71.18	73.01	72.88
TiO_2	1.78	3.05	1.73	1.68	2.86	1.56	0.94	1.58	1.57	2.38	2.54	0.65	0.30	0.28	0.29
Al_2O_3	14.56	13.31	16.07	15.59	13.63	15.62	16.29	15.35	15.41	11.63	9.30	13.81	13.70	13.45	13.51
FeO	12.44	13.57	10.82	11.34	12.46	10.67	9.97	10.10	9.00	9.37	9.60	6.77	3.18	3.20	2.74
MnO	0.18	0.18	0.14	0.15	0.20	0.14	0.18	0.17	0.19	0.13	0.09	0.14	0.03	0.04	0.04
MgO	6.07	3.34	6.11	4.80	3.96	5.53	6.68	4.32	5.16	2.87	2.04	0.42	0.24	0.55	0.44
CaO	5.95	6.02	7.42	9.09	4.40	5.80	4.95	5.65	5.94	10.89	12.66	2.01	0.18	0.53	0.90
Na_2O	4.16	2.87	2.55	2.64	3.20	3.10	3.90	2.96	3.09	1.59	0.08	3.88	2.13	2.82	3.04
K_2O	2.44	3.05	1.66	1.20	2.91	2.09	1.55	3.20	2.13	0.49	0.09	4.52	9.05	6.07	6.12
P_2O_5	0.29	1.41	0.38	0.39	1.18	0.35	0.08	0.42	0.41	0.21	0.22	0.11	0.01	0.05	0.05
Total	100.00	100.00	100.00	100.00	100.00	100.00	100.00	100.00	100.00	100.00	100.00	100.00	100.00	100.00	100.00
AN	28.27	37.27	56.08	54.90	34.28	46.26	40.40	43.36	45.57	63.25	97.19	17.33	4.45	8.80	13.81
Q	0.00	7.95	5.16	6.09	9.56	5.76	1.84	6.70	9.31	25.62	37.33	20.20	22.08	29.67	27.79
or	13.89	17.26	9.46	6.91	16.43	11.94	8.86	18.26	12.17	2.78	0.53	25.88	52.83	35.04	35.46
ab	33.93	23.27	20.82	21.66	25.89	25.39	31.90	24.20	25.30	12.78	0.68	31.82	17.77	23.33	25.22
an	13.37	13.82	26.58	26.37	13.50	21.85	21.62	18.53	21.18	21.99	23.44	6.67	0.83	2.25	4.04
C	0.00	0.00	0.00	0.00	0.04	0.00	0.00	0.00	0.00	0.00	0.00	0.00	0.11	1.36	0.36
di	10.90	4.96	5.33	12.32	0.00	3.11	1.28	4.83	3.83	21.24	16.44	1.99	0.00	0.00	0.00
hy	3.34	13.90	20.91	15.57	16.65	21.10	25.99	16.22	16.89	0.00	0.00	5.96	3.04	3.85	3.15
wo	0.00	0.00	0.00	0.00	0.00	0.00	0.00	0.00	0.00	0.75	6.11	0.00	0.00	0.00	0.00
ol	12.72	0.00	0.00	0.00	0.00	0.00	0.00	0.00	0.00	0.00	0.00	0.00	0.00	0.00	0.00
mt	4.67	6.41	4.60	4.54	6.13	4.36	3.49	4.39	4.38	5.45	5.67	3.09	1.68	1.68	1.44
il	3.27	5.55	3.17	3.10	5.18	2.87	1.73	2.91	2.89	4.29	4.58	1.20	0.57	0.51	0.53
ap	0.65	3.13	0.86	0.88	2.62	0.79	0.19	0.95	0.93	0.46	0.49	0.25	0.02	0.12	0.12
FeO*	12.44	13.57	10.82	11.34	12.46	10.67	9.97	10.10	9.00	9.37	9.60	6.77	3.18	3.20	2.74
F/F+M	0.675	0.805	0.642	0.705	0.761	0.662	0.603	0.704	0.640	0.768	0.826	0.942	0.930	0.854	0.864
den	2.65	2.65	2.64	2.65	2.62	2.61	2.59	2.58	2.57	2.60	2.60	2.42	2.34	2.35	2.34

Appendix E
(Continued)

CIPW Normative Analysis

Sample	MNW-2	BQ-6	BQ-7	JQ-2	MNW-1	MNW-5	MNW-6	JQ-1	MNW-4	JWUN-1	BQ-9	JQ-3	BQ-2	BQ-1	JWUF-1
Group #	3.00	3.00	3.00	3.00	3.00	3.00	3.00	3.00	3.00	3.00	3.00	3.00	3.00	3.00	3.00
Qual	1	5	5	1	1	1	1	1	1	5	5	1	1	1	1
Key	5	5	5	5	5	5	5	5	5	5	5	5	5	5	5
Ref	1	1	1	1	1	1	1	1	1	1	1	1	1	1	1
SiO_2	72.95	73.11	73.44	73.82	73.95	73.80	74.57	74.91	75.05	76.00	75.36	75.92	75.73	76.17	76.76
TiO_2	0.40	0.26	0.26	0.38	0.30	0.30	0.36	0.33	0.35	0.17	0.19	0.23	0.18	0.19	0.16
Al_2O_3	12.42	13.51	13.54	12.16	12.11	12.14	12.05	11.72	11.85	12.25	13.13	11.50	13.08	12.76	11.39
FeO	4.28	2.63	2.17	3.70	3.57	3.25	3.32	3.86	3.22	2.06	1.52	2.72	1.20	1.18	2.46
MnO	0.08	0.04	0.04	0.05	0.06	0.05	0.06	0.07	0.06	0.04	0.02	0.05	0.02	0.01	0.02
MgO	0.81	0.38	0.39	0.53	0.37	0.43	0.42	0.54	0.34	0.08	0.27	0.31	0.18	0.26	0.09
CaO	0.21	0.82	0.92	0.44	0.14	0.14	0.22	0.19	0.21	0.32	0.82	0.13	0.76	0.75	0.20
Na_2O	1.11	3.23	3.17	1.63	1.14	0.84	1.63	1.97	1.77	3.27	3.22	1.03	2.12	2.19	1.69
K_2O	7.70	5.98	6.02	7.24	8.36	9.04	7.33	6.38	7.12	5.81	5.44	8.09	6.70	6.44	7.23
P_2O_5	0.04	0.04	0.05	0.05	0.01	0.01	0.05	0.03	0.04	0.01	0.03	0.02	0.03	0.03	0.00
Total	100.00	100.00	100.00	100.00	100.00	100.00	100.00	100.00	100.00	100.00	100.00	100.00	100.00	100.00	100.00
AN	7.80	12.25	13.59	11.77	6.23	8.22	5.35	4.35	5.03	5.17	12.40	5.68	16.62	15.98	6.56
Q	33.28	27.82	29.03	33.08	32.54	31.76	34.38	35.81	34.88	32.47	33.47	36.70	35.52	36.31	37.25
or	44.68	34.75	34.93	41.96	48.46	52.66	42.67	37.05	41.31	33.51	31.85	47.10	39.06	37.53	42.14
ab	9.22	26.91	26.32	13.54	9.48	7.02	13.54	16.42	14.72	26.99	26.99	8.55	17.69	18.28	14.13
an	0.78	3.76	4.14	1.81	0.63	0.63	0.76	0.75	0.78	1.47	3.82	0.51	3.52	3.48	0.99
C	1.93	0.32	0.26	0.95	0.93	0.73	1.13	1.27	0.93	0.04	0.54	0.84	1.03	0.88	0.41
hy	5.36	2.94	0.95	4.11	3.75	3.58	3.56	4.41	3.27	1.84	0.67	2.94	0.45	0.65	2.23
mt	2.25	1.39	1.79	1.95	1.88	1.72	1.75	2.03	1.69	1.08	0.61	1.43	0.64	0.64	1.30
il	0.74	0.49	0.49	0.70	0.55	0.57	0.66	0.61	0.65	0.32	0.36	0.44	0.34	0.36	0.30
hem	0.00	0.00	0.29	0.00	0.00	0.00	0.00	0.00	0.00	0.00	0.88	0.00	0.50	0.45	0.00
ap	0.09	0.09	0.12	0.12	0.02	0.02	0.12	0.07	0.09	0.02	0.07	0.05	0.07	0.07	0.00
FeOt	4.28	2.63	2.17	3.70	3.57	3.25	3.32	3.86	3.22	2.06	1.52	2.72	1.20	1.18	2.46
F/F+M	0.843	0.877	0.851	0.876	0.908	0.886	0.890	0.879	0.907	0.962	0.850	0.898	0.870	0.818	0.965
den	2.36	2.34	2.34	2.35	2.34	2.34	2.34	2.35	2.34	2.32	2.32	2.33	2.31	2.31	2.32

Appendix E
(Continued)

CIPW Normative Analysis

Sample	LC-3	LC-4	NIO-8
Group #	3.00	3.00	3.00
Qual	1	1	1
Key	5	5	5
Ref	1	1	1
SiO_2	76.93	77.12	77.11
TiO_2	0.15	0.14	0.14
Al_2O_3	11.25	10.71	10.62
FeO	2.07	2.14	2.06
MnO	0.03	0.04	0.02
MgO	0.22	0.08	0.05
CaO	0.13	0.31	0.13
Na_2O	0.57	0.18	0.30
K_2O	8.64	9.27	9.57
Total	100.00	100.00	100.00
AN	11.79	40.30	0.00
Q	38.83	38.73	37.77
or	50.71	54.31	56.44
ab	4.82	1.52	1.30
an	0.64	1.03	0.00
C	0.71	0.00	0.00
di	0.00	0.45	0.57
hy	2.24	1.76	1.82
ac	0.00	0.00	1.09
mt	1.10	1.14	0.35
il	0.28	0.27	0.27
FeO*	2.07	2.14	2.06
F/F+M	0.905	0.964	0.976
den	2.31	2.31	2.31

Appendix F

Least Squares Regression of NIQ-2

Appendix F

Least Squares Regression of NIQ-2

The Parent lava is NIQ-2

Coef	%	
0.146	0.262	OL(US1)
0.302	0.542	BYTOW
0.109	0.196	CHAUG
0.434		LC-2 is the daughter

	SiO2	TiO2	Al2O3	FeO	MnO	MgO	CaO	Na2O	K2O	P2O5
LC-2	55.14	1.56	15.62	10.66	0.14	5.53	5.80	3.10	2.09	0.35
NIQ-2										
OBS	49.39	1.45	16.99	11.43	0.18	7.73	9.45	2.30	0.83	0.26
CALC	49.67	0.74	16.82	11.43	0.15	7.66	9.41	2.16	0.96	0.16
DIF	-0.11	0.71	0.08	-0.00	0.02	0.07	0.04	0.14	-0.13	0.10

Sum of squares of residuals= 0.578

	D	CALC	OBS	RESID	LC-2
RB	0.07	32	9	-23	70
BA	0.16	481	477	-3	970
SR	1.83	929	336	-593	464
V	0.00	0	0	0	0
CR	0.01	40	197	157	92
NI	0.01	39	195	156	89
ZR	0.01	127	137	10	291

Do another one? (Y/N)

Appendix F
(Continued)

Least Squares Regression of NIQ-2

The Hybrid lava is NIQ-10

Coef	%	
0.061	0.061	OL(US1)
0.004	0.004	CHAUG
0.090	0.090	BYTOW
0.720	0.718	NIQ-2
0.127	0.127	MNW-1

	SiO2	TiO2	Al2O3	FeO	MnO	MgO	CaO	Na2O	K2O	P2O5
OL(US	34.67	0.06	0.03	41.27	0.50	23.17	0.25	0.00	0.00	0.05
CHAUG	53.22	0.50	2.82	6.37	0.15	16.49	20.08	0.35	0.01	0.00
BYTOW	49.18	0.00	32.22	0.24	0.00	0.20	15.42	2.58	0.17	0.00
NIQ-2	48.63	1.43	16.73	11.26	0.17	7.61	9.30	2.26	2.35	0.26
MNW-1	73.95	0.30	12.11	3.57	0.06	0.37	0.14	1.14	8.36	0.01

NIQ-10										
OBS	52.34	1.49	15.76	11.08	0.17	6.86	7.87	2.85	1.28	0.29
CALC	51.17	1.07	16.50	11.14	0.16	7.03	8.20	2.01	2.77	0.19
DIF	0.47	0.42	-0.37	-0.06	0.00	-0.17	-0.33	0.84	-1.48	0.10

Sum of squares of residuals= 3.588

Do another one? (Y/N)

Appendix G

Trace Element Partion Coefficients

Appendix G

Trace Element Partition Coefficients

	,OL- 1	CPX- 2	PLG- 3	SPN- 4
NI	12.0000	4.0000	0.0400	6.0000
SR	0.0100	0.1000	2.0000	0.0500
RB	0.0050	0.0200	0.0500	0.0100
Y	0.0100	0.5000	0.0200	0.1000
ZR	0.0100	0.1000	0.0300	0.1000
BA	0.0100	0.0200	0.3000	0.0200
SM	0.0100	0.4000	0.0700	0.0500
LA	0.0050	0.1000	0.1200	0.0300
CE	0.0050	0.2000	0.0800	0.0300
YB	0.0200	0.5500	0.0400	0.1000
LU	0.0200	0.5500	0.0400	0.1000
CR	1.0000	5.0000	0.0400	175.0000
HF	0.0100	0.3000	0.0200	0.0100
TH	0.0010	0.0100	0.0100	0.0050
EU	0.0100	0.5000	0.5000	0.0500
TB	0.0150	0.6000	0.0600	0.0700

Appendix H

Correlation Coefficients with Alteration Indicators

Appendix H

Correlation Coefficients with Alteration Indicators

	Fe2O3	K2O
K2O	-0.545	
Ni	-0.771	
Cu	-0.395	0.456
Zn	-0.099	0.246
Sr	-0.820	0.702
Rb	0.662	-0.549
Y	0.643	-0.463
Zr	0.520	-0.362
Nb	0.319	-0.323
Ba	-0.038	-0.011
Lax	0.016	-0.087
Sm	0.621	-0.520
La	0.630	-0.490
Ce	0.661	-0.507
Yb	0.600	-0.515
Lu	0.622	-0.491
Cr	-0.607	0.696
Hf	0.690	-0.550
Th	0.821	-0.605
Eu	-0.146	-0.094
Tb	0.524	-0.399

MICHIGAN STATE UNIV. LIBRARIES
31293006058535